

TECHNO-ECONOMIC ANALYSIS OF CO₂-EOR OF DEPLETED RESERVOIRS – AN APPLICATION IN THE LOKELE FIELD CAMEROON

Ateh Armstrong Akoteh^{1,2} and Yimen Nasser¹

¹ National Advanced School of Engineering, University of Yaoundé, Yaoundé, Cameroon

² Department of Mechanical, Petroleum and Gas Engineering, National Advanced School of Mines and Petroleum Industries, University of Maroua, P.O. Box 46 Maroua, Cameroon

* Corresponding author: aarmstrongateh@gmail.com

How to cite this paper:

Ateh Armstrong Akoteh,
Yimen Nasser (2025)
Techno-Economic
Analysis of CO₂-EOR of
Depleted Reservoirs – an
Application in the Lokele
Field Cameroon, Journal
of Global Resources, Vol.
11 (02)


DOI:

10.46587/JGR.2025.v11i02.005

Received: 16 May 2025

Reviewed: 12 June 2025

Final Accepted: 28 June 2025


OPEN ACCESS
Freely available Online
www.isdesr.org

Abstract: This work presents a techno-economic analysis of CO₂-EOR of depleted reservoirs, with a focus on its application in the Lokele Field in Cameroon. The study aims to assess the feasibility and potential benefits of CO₂-EOR in the Lokele Field, as well as to identify the key technical and economic factors that affect its viability. The analysis is based on a comprehensive review of the relevant literature, as well as on field data and simulations. The results of the study indicate that CO₂-EOR is a technically feasible and potentially profitable method for enhancing oil recovery in the Lokele Field. The simulations show that injecting CO₂ into the reservoir can increase the recovery factor by up to 25 percent, depending on the injection rate, pressure, and other parameters. The economic analysis suggests significant economic benefits, including a net present value (NPV) of 1445 (USD million), a payback period (PBP) of 5.54 years, and an internal rate of return (IRR) of 25.69 percent. However, the analysis also reveals that the viability of the project is highly sensitive to key factors such as the Capital cost, discount rate, the oil price and the gas price. The study concludes that CO₂-EOR can be a viable and attractive option for enhancing oil recovery in depleted reservoirs, including in the Lokele Field. However, its success depends on a range of technical, economic, and regulatory factors that need to be carefully considered and managed. The study suggests that further research and field testing are needed to refine the models and assumptions used in the analysis and to validate the findings.

Keywords: CO₂-EOR, Depleted Reservoirs, Techno-Economic Analysis, Payback Period (PBP)

Introduction

High concentration of CO₂ generated by industries only increase over the years. According to the Journal of the United Nation Framework Convention on Climate Change (UNFCCC) published on March 9 2022, the global energy-related carbon dioxide emissions increased by 6 percent in 2022 to attend 36.3 billion tons of their highest level never achieved [1]. These amounts emitted must draw the attention of states to make important decisions for the preservation of nature. Enhanced oil recovery (EOR) techniques are increasingly being used to increase oil production from depleted reservoirs. One such technique is the injection of carbon dioxide (CO₂) into the reservoir to enhance oil recovery. CO₂-EOR not only increases oil production but also helps to reduce greenhouse gas emissions by storing CO₂ in the reservoir. The Lokele field in Cameroon has the potential to be a promising candidate for CO₂-EOR. This paper aims to conduct a techno-economic analysis of CO₂-EOR in the Lokele field in Cameroon. Many studies have proposed optimization models at various stages of the production process. However, unlike those studies CCUS technology is an approach in optimizing oil recovery while reducing CO₂ emissions. Daniel p. Arnold et al in their work used CCUS technology for optimization of CO₂ recycling operations in pre-salt carbonate reservoirs and as a result yielded a lower carbon footprint with reduction of operational emissions and increase in the NPV [2], in [3], several aspects of CO₂ injection for both oil recovery and CO₂ storage were discussed. They assumed in their simulations that gas was first contact miscible and gas-liquid relative permeabilities were made straight lines with endpoint values of 1.. In [4] CCUS technology was used to develop an optimization-based assessment framework that aims to incorporate CO₂ storage and utilization into an integrated framework and their results showed that adsorption is the preferred capture technology at relative high flue gas rate and CO₂ concentration. In a simulation study of the injection strategy and operational parameters on both CO₂ sequestration and enhanced gas recovery, Jikich et al. [5] found that injecting CO₂ at a higher pressure via horizontal wells helps store CO₂, but reduces methane recovery. Based on their simulation results, CO₂ injection can yield the highest methane recovery after primary recovery. Carbon emissions in Cameroon are projected to increase such that by 2043 the total amount of CO₂ released will be 15.1 million tons [6]. Due to this, Cameroon has submitted his Nationally Determined contribution (NDC) in October 2015 of its target in reducing greenhouse gas (GHG) emissions, putting into place several cash projects to reduce 35 percent carbon footprint by 2030 such that the total cost of investment is evaluated to be 28,713 billion CFA [7]. The field of our study is that of Lokele exploited by a Company Located at Mokoko Abana in Cameroon so its total production is estimated at 5,544,460bbl in 2015 [8]. The reservoir consists of grid blocks and 11 wells to which the production began in 2000 and reached its decline in 2017. During this period the annual production evaluated for the gas is 106,546,000 m³ and for the oil of 3,536,630 m³. Moreover, a huge amount of gas was burned at the torch due to the excess production of gas. Thus, in view of government's policy on global warming, what technique can we use to reduce our CO₂ emissions in tertiary recovery of hydrocarbons (CO₂-EOR) while making economic and even environmental profits?

The techno-economic analysis of CO₂-EOR of depleted reservoirs in the Lokele field in Cameroon involves evaluating the feasibility and profitability of implementing CO₂ enhanced oil recovery (EOR) techniques in the field. This involves a detailed analysis of the costs and benefits associated with implementing this technology as well as the potential environmental impact. The analysis typically includes the following steps:

Identification of key parameters: Key parameters that impact the feasibility and profitability of CO₂-EOR in the Lokele field are identified, such as the size and quality of the reservoir, the current oil recovery rate, the available CO₂ sources, the cost of CO₂ transportation and injection, and the potential environmental impact.

Evaluation of CO₂ sources: Various CO₂ sources are evaluated, such as natural CO₂ deposits, industrial CO₂ emissions, and anthropogenic CO₂ captured from the atmosphere. The cost and availability of each source are assessed.

Design of CO₂-EOR operations: The CO₂-EOR operations are designed based on the identified key parameters and CO₂ sources. The design process includes the selection of the injection rate, injection pressure, and production rate, as well as the determination of the required amount of CO₂.

Cost analysis: The cost of implementing CO₂-EOR in the Lokele field is estimated, taking into account the costs of CO₂ capture, transportation, injection, and monitoring. The costs of equipment and labor are also included.

Economic analysis: The economic benefits of CO₂-EOR are evaluated, such as the additional oil production, the increased revenue, and the potential tax benefits. The analysis also considers the impact of the technology on the price of oil and the competitiveness of the Lokele field in the global market.

Environmental impact assessment: The potential environmental impact of CO₂-EOR in the Lokele field is evaluated, such as the impact on the local ecosystem, water resources, and air quality. The analysis also considers the potential long-term impact of CO₂ emissions on the global climate.

By conducting such a techno-economic analysis, decision-makers can better understand the feasibility and profitability of CO₂-EOR in the Lokele field and make more informed decisions regarding the implementation of this technology.

Material and Methods

Carbon dioxide enhanced oil recovery (CO₂-EOR) is a process of injecting carbon dioxide into depleted oil reservoirs to increase the production of oil. This process has gained significant attention in recent years as it not only increases oil production but also reduces carbon dioxide emissions by storing the gas underground. The techno-economic analysis of CO₂-EOR involves evaluating the costs and benefits of the process from a technical and economic perspective.

Technical Analysis:

The technical analysis of CO₂-EOR involves evaluating the feasibility of the process and the technical requirements for successful implementation. The following are some of the key technical aspects of CO₂-EOR:

Reservoir Characterization: The success of CO₂-EOR depends on the characteristics of the reservoir, including its porosity, permeability, and oil saturation. A detailed reservoir characterization is required to determine the suitability of the reservoir for CO₂-EOR.

Injection and Production Wells: CO₂ is injected into the reservoir through injection wells, and the oil is produced through production wells. The design and construction of these wells are critical for the success of CO₂-EOR.

CO₂ Source and Transport: The source of CO₂ and the transport infrastructure are critical for the success of CO₂-EOR. The CO₂ can be sourced from industrial processes or from natural sources such as geological formations. The transportation infrastructure should be able to transport the CO₂ from the source to the injection site.

Monitoring and Control: The injection and production process should be continuously monitored and controlled to ensure the success of CO₂-EOR. This includes monitoring the injection pressure, temperature, and flow rate, as well as the production rate of oil.

Economic Analysis: The economic analysis of CO₂-EOR involves evaluating the costs and benefits of the process. The following are some of the key economic aspects of CO₂-EOR:

Capital Costs: The capital costs of CO₂-EOR include the costs of constructing the injection and production wells, the CO₂ source and transport infrastructure, and the monitoring and control systems.

Operating Costs: The operating costs of CO₂-EOR include the costs of injecting the CO₂, monitoring and controlling the process, and producing the oil.

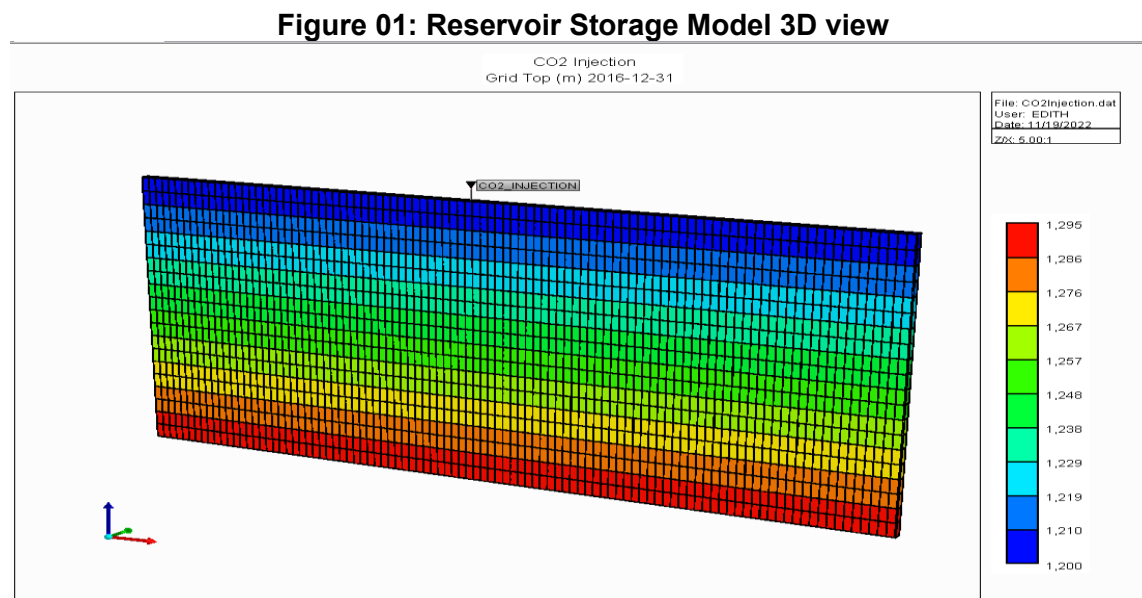
Revenue: The revenue from CO₂-EOR comes from the increased production of oil. The revenue depends on the price of oil and the amount of oil produced.

Carbon Credits: CO₂-EOR can generate carbon credits, which can be sold in carbon markets. The revenue from carbon credits can offset the capital and operating

Model Description

Reservoir Model Description

In this work, a compositional simulation model was built using CMG GEM module. To per-characterize and per-evaluate the CO₂ storage capacity in the Lokele depleted oil reservoir, a heterogeneous box-shaped model consisting of 2000 grids, with grid blocks of 100 × 1 × 20 and corresponding dimensions of 5 × 143 × 1200 ft. Fig.1 displays the reservoir model used in this study in 3D.



Reservoir Rock and Fluid Properties

Reservoir rock properties used for the simulation are shown in the Table 1 below:

Table 01: Table of reservoir rock and fluid properties for carbon storage [54]

Parameter	Value
Reference depth(m)	1200
Grid thickness(m)	5
Porosity(md)	0.12
Permeability(md)	100
Rock Compressibility(1/psi)	5.5e-7
Reference Pressure(psi)	11800
Reference temperature	25°C
Thermal Expansion Coefficient	0.1/C
Atmospheric Pressure of CO ₂	72.8
Critical temperature	304.2
Acentric factor	0.225
Molar weight	44.01

Mathematical Formulations

Equation of State (EOS)

The Peng-Robinson equation of state (commonly referred to as PR-EOS) model is the principal method used in CMG-GEM compositional simulation for phase equilibrium calculation. CO₂ molecular diffusion coefficient will directly affect the penetration depth and injection gas saturation distribution in the reservoir. PR-EOS model is a typically basic model used in petroleum industries. In this case, we describe the phase behavior of solvent(s) - CO₂ oil systems using this PR-EOS model as the equation of state. The PR-EOS model can be expressed as:

$$P = \frac{RT}{V-b} - \frac{a\alpha}{V(V+b)+b(V-b)} \quad (1)$$

Where:

$$a = \Omega_a \frac{R^2 T_c^2}{P_c} \quad (2)$$

$$b = \Omega_b \frac{RT_c}{P_c} \quad (3)$$

With $\Omega_a = 0.45724$ and $\Omega_b = 0.07780$

$$\alpha = [1 + m(1 - \sqrt{T_r})]^2 \quad (4)$$

$$m = 0.3795 + 1.54226\omega - 0.1644\omega^2 + 0.016667\omega^3 \quad (5)$$

Where: R is the ideal gas constant, T is the temperature, T_c is the Critical Temperature, T_r is the Reduced Temperature, V molar Volume, a coefficient in PR-EOS for mixture effects

Viscosity

In order to calculate the viscosity of the reservoir fluids, Pedersen's correlations were used as shown in the equation.

$$\frac{\mu_{mix}(P,T)}{\mu_o(P_o,T_o)} = \left(\frac{T_{c,mix}}{T_{c,o}}\right)^{-1/6} \left(\frac{P_{c,mix}}{P_{c,o}}\right)^{-2/3} \left(\frac{MW_{mix}}{MW_o}\right)^{-1/2} \left(\frac{\alpha_{mix}}{\alpha_o}\right) \quad (6)$$

Where:

μ = Viscosity,

T_c = Critical temperature,

P_c = Critical Pressure,

MW= Molecular Weight,

α = Rotational coupling coefficient.

The subscript "mix" represents the mixture property, and the subscript "o" refers to the reference substance property. The molecular weight of the mixture is calculated with the following equation

CO₂ Solubility

Either Henry's Law or flash calculation methods can be used to model the solubility of fluid components into others in GEM [58].

Henry's Law

$$p\phi_i = H_i x_i \quad (7)$$

Where:

p= Pressure

p_{ref} = Reference pressure

ϕ_i =Fugacity coefficient of component

H_i = Henry's law constant for component

Permeability and Pressure

In the model, the relative permeability and capillary pressure figures were digitized from the data fitted using Corey function and used in the reservoir simulation model. The fitting for drainage and imbibition relative permeability curves is calculated. The saturation of connate water and critical water was defined the Corey coefficient for drainage and imbibition gas curves (C_g), for drainage water curve it was three and for the imbibition water curve (C_w). 'E3W+ The formulas of the relative permeability and the capillary pressure were as follows:

$$k_{rg} = k_{rgmax} \left[\frac{1 - S_w - S_{gcr}}{S_w - S_{gcr}} \right]^{C_g} \quad (8)$$

Where:

S_w is the water saturation, S_{wi} is the initial water saturation, S_{gcr} is the critical gas saturation and C_g is the Corey gas exponent. Moreover, the following is the case:

$$k_{rw} = k_{rwmax} \left[\frac{S_w - S_{wcr}}{S_{wmax} - S_{wcr}} \right]^{C_w} \quad (9)$$

Where:

S_w is water saturation, S_{wmax} is the maximum water saturation, S_{wcr} is the critical water saturation and C_w is the Corey water exponent.

$$P_c = \frac{C_w}{\left(\frac{S_w - S_{wcr}}{T - S_{wcr}} \right)^{a_w}} + \frac{C_g}{\left(\frac{S_g - S_{gr}}{T - S_{gr}} \right)^{a_g}} \quad (10)$$

S_w is the water saturation, S_{wcr} is the critical water saturation, S_g is the gas saturation, S_{gr} is the critical gas saturation, S_w is the water saturation [59].

CO2 Utilisation for Enhanced Oil Recovery

Reservoir Properties

A Black Oil and Unconventional Simulator (IMEX) developed by CMG is used for reservoir modeling and development simulations. History matching simulations are performed using the reservoir's heterogenous properties. A comprehensive description of the reservoir can be found in the table that follows.

Table 02: Table of reservoir rock and fluid properties for EOR [54]

Reservoir Parameters	Value
Oil density (kg/m ³)	945.542
Gas density/gravity(kg/m ³)	0.7
Water phase density(kg/m ³)	995.476
Formation volume factor	1.01112
Temperature	50°C
Rock compressibility(1/kPa)	7.25e-6
Reference pressure(kPa)	20000
Reference depth(m)	1605
Bubble point pressure (KPa)	9000
Viscosity(cp)	0.613465
Water oil contact(m)	1750

Governing Equations

CO₂ solubility in oil

There are numerous important elements that affect carbon dioxide's solubility in oil. The solubility of CO₂ decreases with temperature but increases with pressure and API gravity. Furthermore, oil composition and liquefaction pressure also affect solubility if reservoir temperature falls below the crucial carbon dioxide temperature (T_c , CO₂ = 88°F). When carbon dioxide becomes more soluble, the viscosity of the oil decreases, making supercritical CO₂ injection more effective than subcritical temperature injection. Oil swelling, oil viscosity, and carbon dioxide solubility can all be determined by correlations. Therefore, the following connection can be used to compute the CO₂ solubility for super-critical circumstances [60]:

$$CO_2Solubility \left(\frac{mol}{mol} \right) = 2.238 - 0.33y + 3.23y^{0.6474} - 4.8y^{0.25656} \quad (11)$$

$$\text{With } y = \gamma \left(\frac{T^{0.8}}{P_s} \right) \exp \left(\frac{1}{MW} \right) \quad (12)$$

As for the sub-critical conditions, the correlation is as follows:

$$CO_2Solubility \left(\frac{mol}{mol} \right) = 0.033 - 1.14y + 0.7716y^2 - 0.217y^3 - 0.02183y^4 \quad (13)$$

With

$$y = \gamma \left(\frac{P_s}{P_{liq}} \right) \exp \left(\frac{1}{MW} \right) \quad (14)$$

γ is the oil specific gravity (oil density at 15.6 °C), T is the temperature (F), P_s is the saturation pressure (psi), P_{liq} is the CO₂ liquefaction pressure at the specified temperature (psi), MW is the oil molecular weight, and μ_i is the initial dead oil viscosity at the specified temperature (cp).

Oil swelling

Usually, oil swelling is determined by using the following equation:

$$\text{Oil swelling factor} = \frac{\text{Saturated CO}_2 \text{ volume at current } T}{\text{Oil volume at current } T} \quad (15)$$

In addition to carbon dioxide solubility, oil molecules' size has effect on oil swelling. Apart from equation (15), following correlations can be used to determine oil swelling factor:

Oil viscosity

In addition to carbon dioxide solubility, oil viscosity during Immiscible-CO₂ EOR is dependent on pressure. So, as saturation pressure increases, viscosity decreases until the pressure reaches liquefaction value, after which it starts to rise as the result of pressure and oil compressibility [54].

Following equation can be used to determine oil viscosity during Immiscible-CO₂ EOR:

$$\text{Oil viscosity} = \gamma \mu_i - 10.8 \left(\frac{\text{CO}_2 \text{ solubility}}{\mu_i} \right) \quad (16)$$

$$\text{With } \gamma = x^{-0.74} \text{ and } \left[\mu_i \left(\frac{P_s}{\mu_i} \right)^{0.2} \right]^{\frac{\gamma}{\text{CO}_2 \text{ solubility}}} \quad (17)$$

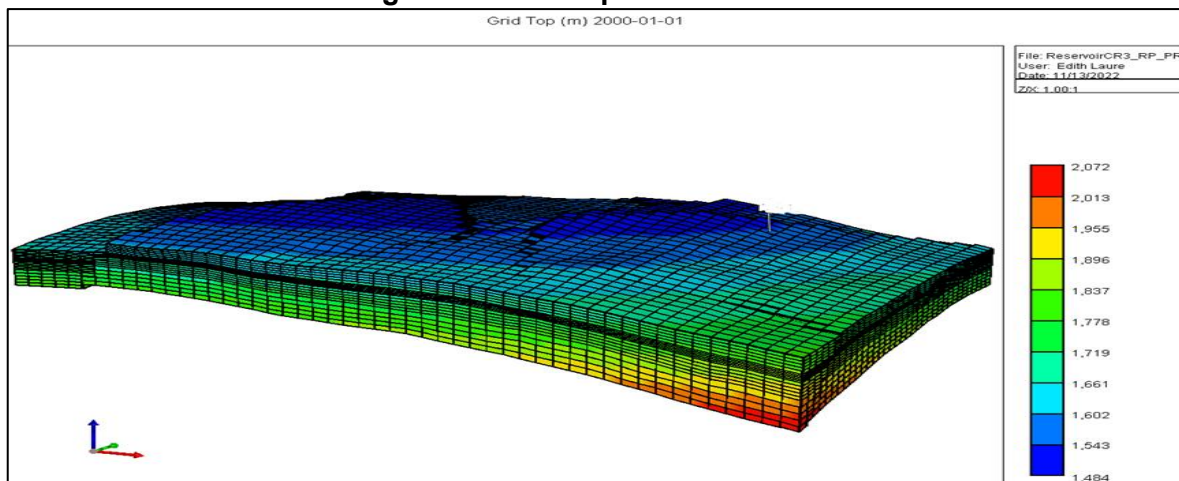
P_s is the saturation pressure (psi), and μ_i is the initial dead oil viscosity at the specified

Reservoir Simulation

Static Reservoir Model

This model is described on a simple three-dimension Cartesian grid model with a total of 35000 grid cells, its geological structure contains 12233 view blocks and 18842 exterior faces. The reservoir model has a dimension of 50ft x 35ft x 20ft in the X, Y, Z respectively. The reservoir is divided into 20 layers with a water oil contact (WOC) of 1750m, and data file of porosity and permeability. The saturation profile of our reservoir clearly shows its heterogeneity. The grid top value ranges from 1484 to 2072m as seen in Figure 2 below. The porosity and permeability profiles are also visualized, thus highlighting the heterogeneity of our chosen CMG IMEX Model. Fig.2 represents our reservoir in the grid top block form where the red indicates the highest depth, the yellow and green averagely high and the blue the surface.

Figure 02: Grid top of the Reservoir



Dynamic Reservoir model

Dynamic reservoir modeling has been carried out using the black-oil simulator CMG-IMEX. The field is made up of 11 production wells namely PIA, PIB, PIC, PID, PIE, PIF, PIG, PIH, PII, PIJ, PIK. History matching of the primary and secondary recovery phases is carried out before validating the model with current CO₂ injection data. The production wells are operated under a maximum liquid rate of 3324 stb/day, provide pressure support for oil displacement and are operated under a 9000 kPa bubble point pressure. The reservoir was initialized to be in equilibrium with no gas cap because the original reservoir pressure was above the bubble point pressure. The well produces for a period of 17 years.

Economic Model of CCS AND CO₂ – EOR

This section presents the economic analysis used to evaluate the feasibility of a CO₂ – EOR project. Cost models include amortized capital costs, operating and maintenance costs, and other costs. There are many methods to assess CO₂-EOR project costs, including, in order of increasing complexity and data requirement, empirical model, budget model, and final accounts. Investment decisions on CO₂-flooding projects rely on budget models, which depend on project design and market price.

Cost Model

The four key cost types for the CCS project in this study are capital costs, CO₂ capture costs, operation and maintenance (O&M) costs, and abandonment costs. The capital costs are incurred at the outset of the project according to the cost model. The gas field, compressor, pipeline, wells, and injection platforms are all included in the capital cost. Using the project discount rate, these capital expenses are amortized throughout the field's lifetime [52]. According to the gas field's requirements, which include the processing equipment, production equipment, injection platforms, wells, and transportation pipeline, the cost of CO₂ capture is estimated. The capital expense for putting the chosen CO₂ capture technology into use for the CCS project is known as the CO₂ capture cost. O&M expenditures include labor for site operation and maintenance (surface and subsurface), services, consumables, and general administrative needs [53]. The expenses in this study were calculated based on research reports from earlier studies as well as studies carried out by respected organizations including the Asia Pacific Economic Cooperation (APEC), CO₂CRC, IEAGHG, and GCCSI [61].

All price statistics have been changed to reflect constant 2020 US Dollar (USD):

$$PV = \frac{FV}{(1+i \text{ percent})^n} \quad (18)$$

Whereby, PV is present value, FV is future value, i is discount rate, and n is the project lifetime number of years.

Table 03: Key Economic Assumptions and References in this Study [61]

Input Data	Data
Year Enacted	2020
Project lifetime (N, year)	14
Interest rate (percent)	3
Discount rate (R, percent)	8
Plant capacity (MMscf/d)	440
Gas price (\$/MMBtu)	2.8
Oil price (\$/bbl)	81.38
CO ₂ price (\$/tonne)	23
Capital cost USD Million	427.9
CO ₂ capture technologies cost (USD Million)	410
Tax (percent)	38 percent
Operation and maintenance cost (percent)	2.5
Abandonment cost (USD Million)	50

Cost Evaluation Metrics

Net Present Value (NPV)

Over the course of the CCS project's lifetime, future cash flows are accrued incrementally as well as cumulatively, and this value is represented by NPV.

To account for the time value of money and the risks/uncertainties related to future cash flows, the total value of cash inflows and outflows is what is discounted.

To create NPV estimates in time series, net revenues (cash inflows) from the revenue model were combined with total expenses (cash outflows) computed by the cost model (years). When estimating the CCS project profitability at the end of its lifespan, the cumulative net present value (NPV) is computed. Positive values indicate profit possibilities, while negative values represent financial losses incurred by project stakeholders and investors. If $NPV > 0$, the project is deemed feasible, and vice versa. The NPV computation is shown as follows [62]:

$$NPV(i, N) = \sum_{t=0}^N \frac{C_t}{(1+i)^t} \quad (19)$$

Whereby; i is the discount rate, C_t the annual cash flow in the t the year, and N is the total number of years. Time period $t = 0$ relates to the investment during the project lifetime.

Payback Period (PBP)

PBP is a representation of the amount of time required to recover the capital expenditure that was initially spent in a CCS project. According to the estimates, the project's fiscal viability strength will rise when the PBP value decreases and vice versa. Moreover, the year that the computed cumulative cash flow turns positive and reaches breakeven is used to define PBP. Below is how the PBP is expressed [62]:

$$PBP = 1 + A - \frac{B}{C} \quad (20)$$

Whereby; A is the final year with negative cumulative cash flow, B is the value of cumulative cash flow at the end of year A , and C is the total annual cash flow during the year after A .

Internal Rate of Return (IRR)

IRR could be used to measure the total investment and profit gain in the CCUS project. According to the calculations, the project gain will grow as the IRR value grows, and vice versa. Furthermore, the project cash flow net present value (NPV) is being reduced to zero (0) by the discount rate value, which establishes the lowest rate of return necessary to make the project viable. The CCS project is deemed feasible if the realized internal rate of return (IRR) exceeds the specified discount rate. The computed and displayed IRR is:

$$NPV(IRR, N) = \sum_{t=0}^N \frac{C_t}{(1+IRR)^t} = 0 \quad (21)$$

Whereby; i is the discount rate, C_t the annual cash flow in the t the year, and N is the total number of years. Time period $t = 0$ relates to the investment during the project lifetime.

Results and Discussion

The study aims to assess the feasibility and potential benefits of CO₂-EOR in the Lokele Field, as well as to identify the key technical and economic factors that affect its viability. The analysis is based on a comprehensive review of the relevant literature, as well as on field data and simulations. We obtained results from the capturing process of atmospheric CO₂ by explaining the process flow on Aspen plus software, then for storage and utilization for EOR in the CMG software based on the different steps and scenarios as will be analyzed in this part.

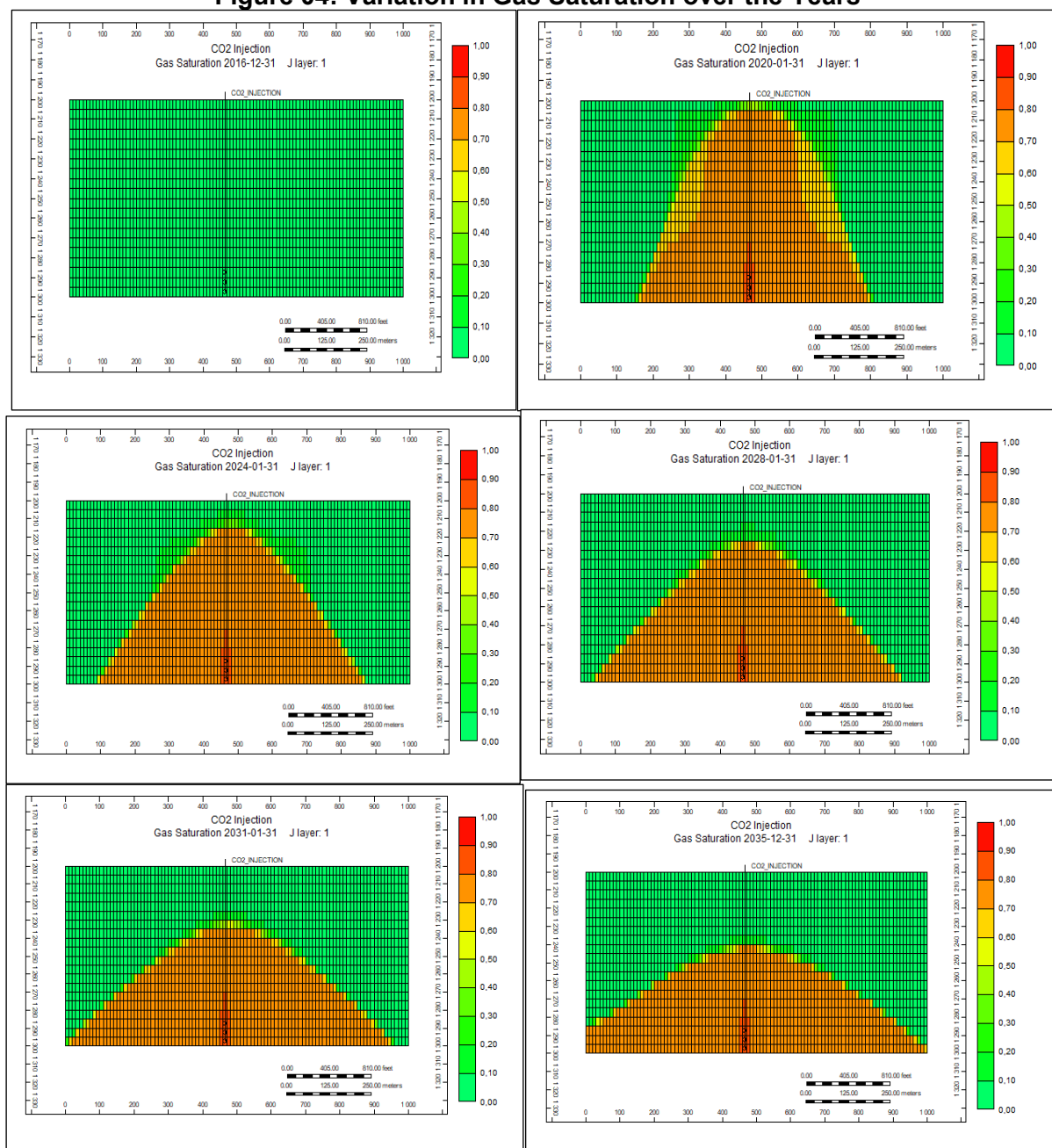
Carbon Storage

The use of a depleted reservoir with a capacity of 171,600,000m³ still located in the Lokele field, consisting of a single layer with 2000 grid blocks and a depth of 1200m with porosity 12 percent and permeability of 100mD. This permitted us to place an injection well at the

extremities of the reservoir with coordinates $x=52$, $y=1$, $z=1$ with a depth of 1295m. This well permitted us to inject gas and visualize its propagation between 2016 to 2035 in the reservoir all these with the aid of the Builder tool and the GEM simulator from CMG.

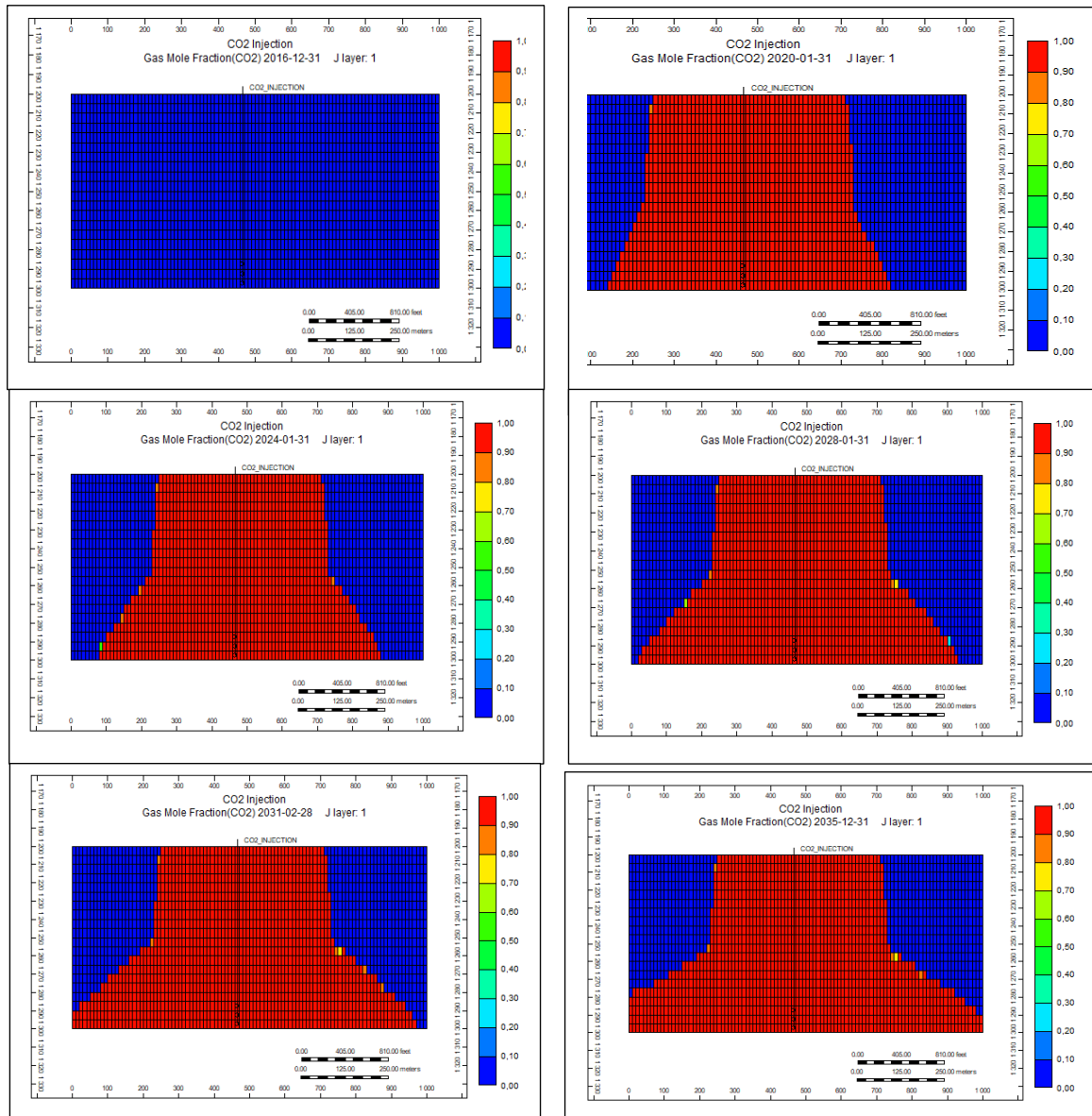
Fig. 4 presents the evolution of the gas saturation in the reservoir. Considering 2016 as the first injection date into this depleted reservoir, we notice that there is no presence of gas in our reservoir and this is materialized by the green color. Storage begins effectively in 2017 and all the 37,000,000m³ of CO₂ is stored all at once. CO₂ stored will spread out progressively to create an oil/CO₂ interface from 2016 to 2035, with gas saturation leaving from 0 percent (green color) to 70 percent (orange color) around our well. In tertiary recovery, CO₂ been miscible with oil by thermodynamic exchanges will gradually break capillary forces and thereby favor the drainage of residual oil towards production wells. The quantity of gas injected does not occupy the entire surface of the reservoir, so we can still increase the flow rate of gas the more and more.

Figure 04: Variation in Gas Saturation over the Years



After having known the volume of gas injected resulting from gas saturation, we will quantify the molar fraction injected into the reservoir. The latter makes it possible to know the quantity of CO₂ molecules present during the storage phase. Fig. 5 shows us that during the first year (2016), the molar fraction is zero materialized by the blue color, and gradually increases up to 2035 leaving from 0 percent to 80 percent

Figure 05: Variation in CO2 Mole Fraction Rate in till 2035

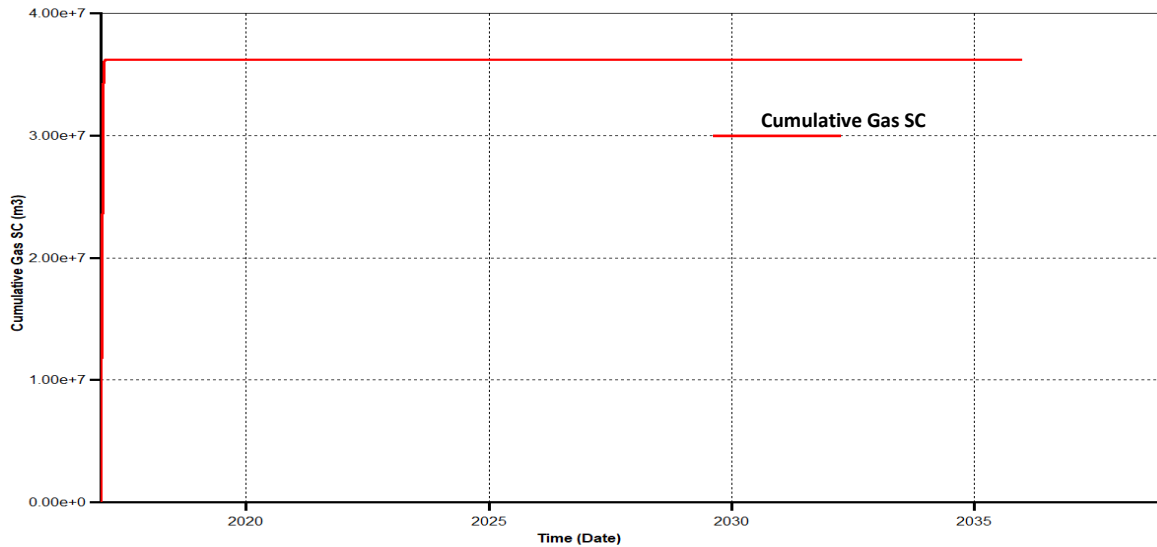


Thanks to the mole fraction, the amount of injected gas can be known. Fig. 6 shows the net amount of stored CO₂ which is 37,000,000m³ in the reservoir from 2016 to 2035 issued from the capture of CO₂ in the atmosphere. Presented in the form of a curve, we have along the x-axis the time and the y-axis the cumulative volume of gas injected (Cumulative Gas SC (m3)). Thus, we note that:

- Between 2016 and 2017, CO₂ is stored at once in the reservoir, the curve increases rapidly passing from 0 to 37,000,000m³, this is due to the calculation speed of the injection and the volume injected as seen in Fig.IV.2 and Fig.IV.3. The gas flow occupies about half of the reservoir.
- Between 2018 and 2035, the volume of gas rate remains constant at 37,000,000m³ meaning the volume of fluids injected into the reservoir is identical at standard pressure

and temperature. Thus, the quantity of gas injected into our reservoir can further be increased.

Figure 6: Cumulative Field CO₂ injection for Storage with Respect to Time



Tab. 4 shows the values of the gas volume flowrate issued from Fig. 6 with respect to time. The storage is carried out at once as from 2017, after which there's no longer injection of the gas for storage that is why in the long run the quantity stored remains constant. Tab.4 shows the amount of CO₂ stored in the reservoir and will help to better effectuate or carry out CO₂ injection in the continuation of our work.

Table 04: Identification of injected Gas flowrate within different years

DATE	2016	2017	2035
GAS FLOW (m ³)	0	37,000,000	37,000,000

CO₂ Utilisation for Enhanced Oil Recovery

Scenario 1: Reservoir model

In this portion of creating a reservoir model, we would visualize the reservoir parameters and production data.

Relative permeability

Relative permeability is defined as the permeability of one phase relative to another when two or more fluids flow together. It is an important factor since it determines the mobility ratio and the Injectivity of the CO₂ in a CO₂ storage process for EOR.

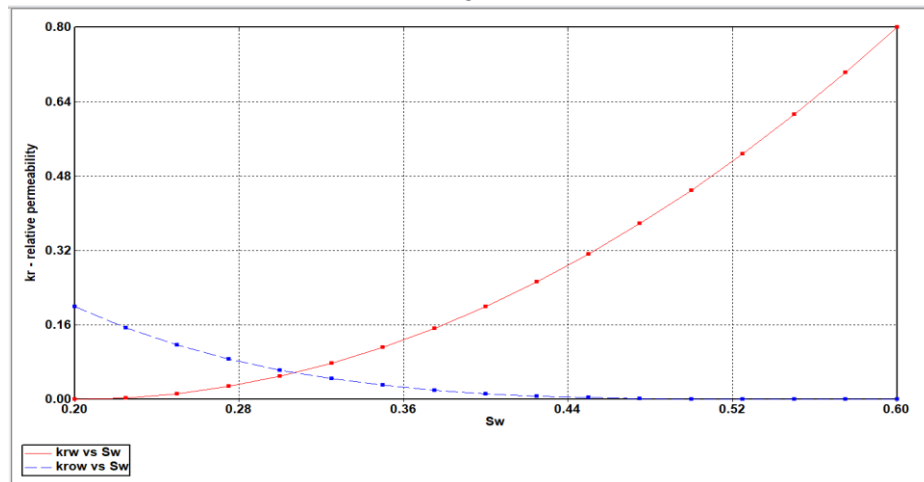
The Fig.7 and 8 represents the relative permeability curves. It informs us about the evolution of saturations of the different phases of our fluid and its evolution during production.

Water-Oil Relative Permeability

Fig.7 shows the water-oil relative permeability on the y-axis as a function of water saturation of our reservoir. We can see here that the relative permeability of water is higher than that of water-oil. The more this permeability in water-oil decreases that of water increases. This increase in water permeability results in the water saturation becoming more important than that of oil after the critical point. At the critical point, the water saturation of water and oil are equal. In reservoirs where oil is the wetting fluid, the increase in relative water permeability is greater than reservoirs where water is the wetting fluid. In analyzing the curve below, we note that it satisfies Craig's conditions listed in appendix 1. In Fig.7 the interstitial water saturation

appears at $S_w = 0.20$ and the point of intersection between the two curves is at $S_w = 0.31$. Taking into account Craig's conditions in appendices 1, we can conclude that in this reservoir, the wetting fluid is water.

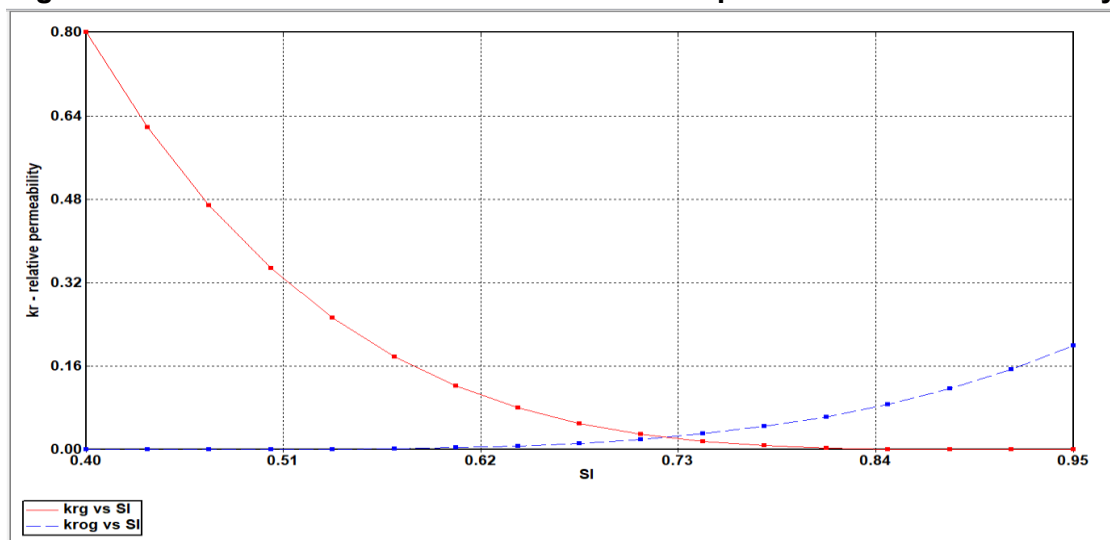
Figure 07: Water-Oil Relative Permeability Curve with Respect to Water Saturation



Gas-oil relative Permeability

Fig.8 below shows the relative permeability curves of the gas and that of the oil-gas on the y-axis as a function of initial saturation on the x-axis. We can observe here that the relative permeability of gas is higher than that of oil-gas. Moreover, the relative permeability of the oil-gas increases while that of gas decreases. This increase in the oil-gas relative permeability has as consequence that the initial saturation becomes more important than that of gas after critical point. At critical point, the oil-gas and gas saturations are equal. By analyzing the curve below, we note that the relative permeability of the oil-gas is very low. The initial saturation appears at $S_i = 0$ and the point of intersection between the two curves is at $S_i = 0.71$. Taking into account the above results, the wetting phase here is the oil and generates the flow of gas. The fluid produced will be mostly oil.

Figure 08: Gas-Oil Initial Saturation Curve With Respect to Relative Permeability

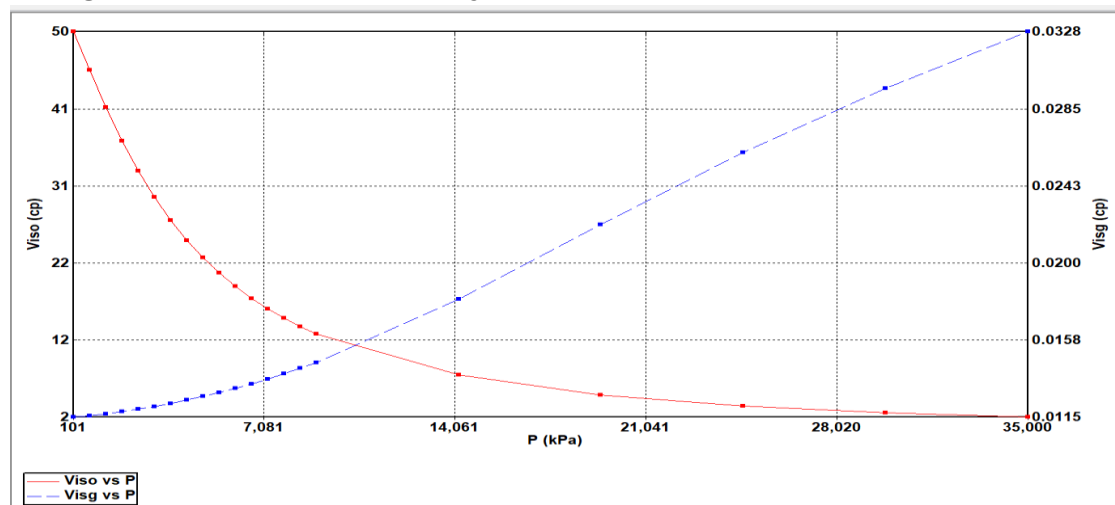


Viscosity

Fig.9 shows oil and gas viscosity curves on the y-axis as a function of the reservoir pressure. We can see here that the oil viscosity is higher than that of gas. In addition, the oil viscosity

decreases while that of gas increases. This increase in gas viscosity creates a reservoir pressure that becomes important than that of oil after the critical point. In a reservoir when the oil viscosity is higher than that of gas, we can say that that our reservoir is of type “black oil”.

Figure 9: Oil and Gas Viscosity Curve with Respect to Reservoir Pressure



Comparative study of models based on production and pressure data

Production and pressure data were used to determine the well derivability thus will permit to identify the best model for our prediction.

- Simulation data versus historical data based on production.

Fig. 10, Fig. 11 and Fig. 12 presents oil, gas and water cut production in the entire field and is based on two curves; that in red (reservoir) comes from the results gotten from the simulation of the reservoir model and that in blue is based on historical data (Prod-History.fnf). Fig. 10 and Fig. 11 presents the evolution in the production of oil and gas so the curves vary as follows:

- Between 2000 and 2003 the production of oil and gas is increasing but the two models are not superposed
- Between 2003 and 2007 the production of oil and gas drops rapidly but the two models get closer to each other.
- In 2007 the production of oil and gas attends its decline and for the oil rate, the two curves are closer while for the gas rate the two curves are far apart.

This implies that the simulation model we have is not the ideal model for this reservoir because they are not closer to that of the production history of the well.

Figure 10: Oil rate produced based on historical and simulation model data

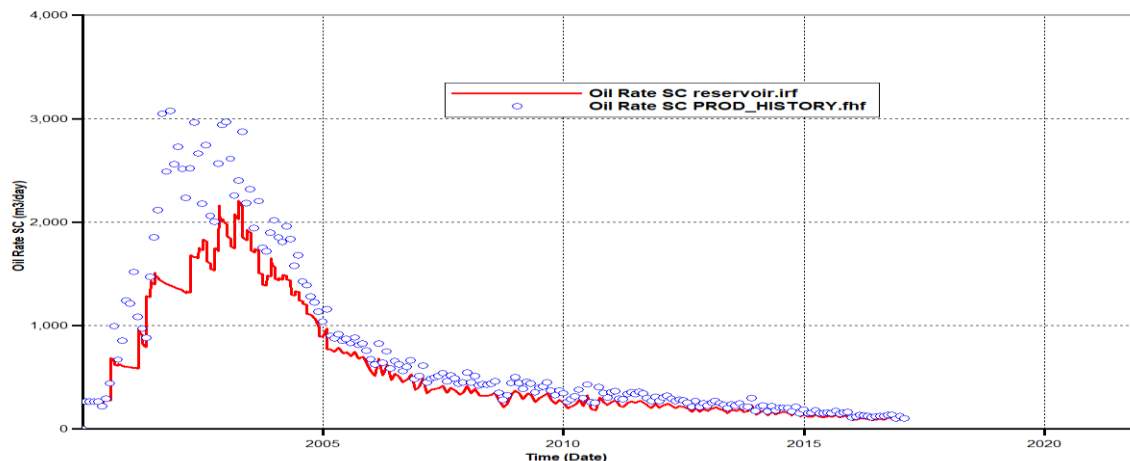


Figure 11: Gas rate produced based on historical and simulation model data

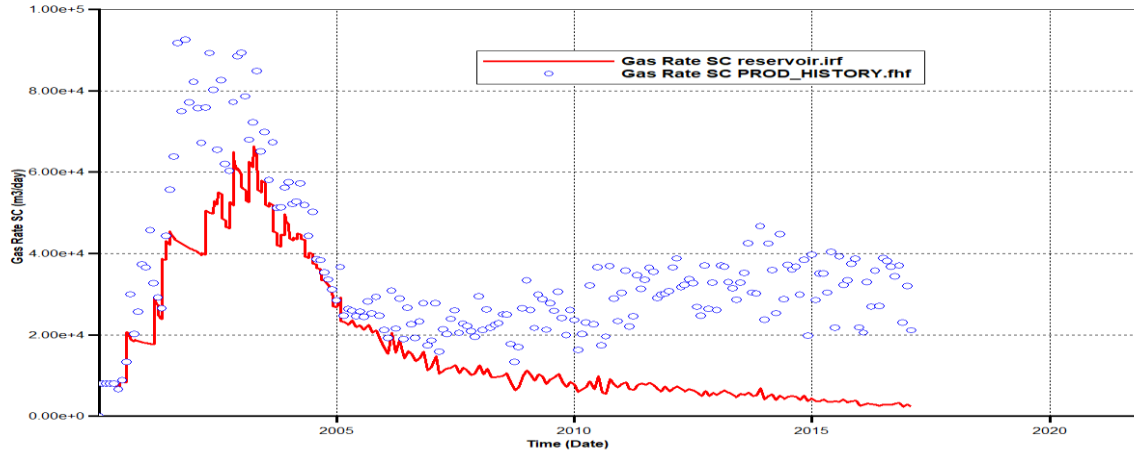
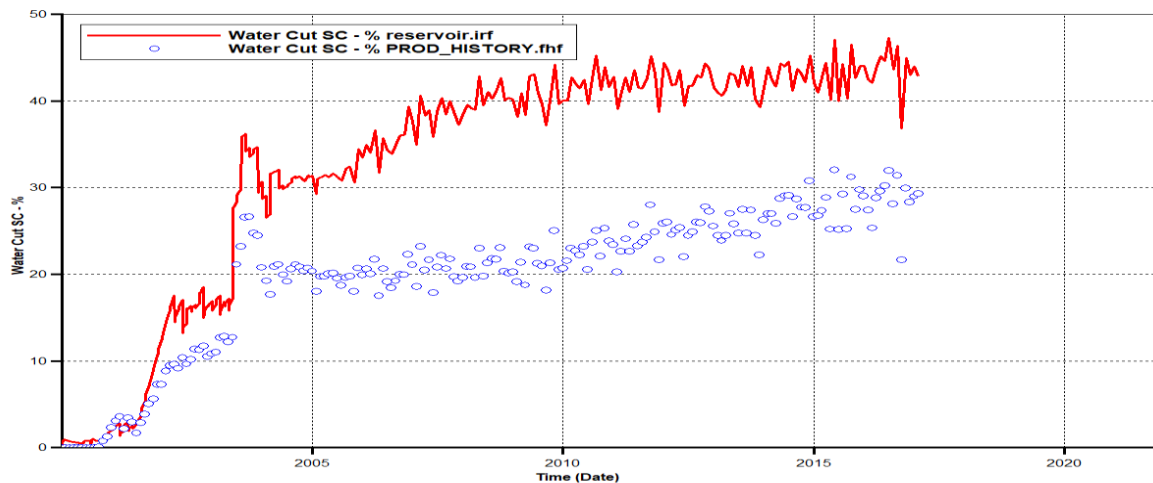


Fig.12 presents the evolution of water cut with respect to time where the simulation data is represented in red (reservoir.irf) and historical data is represented in blue (PROD-HISTORY.fnf). We observe here that the water cut curve of the simulation model is higher than that of the production history curve, showing that the two curves are not superposed.

Figure 12: Water cut rate produced based on historical and simulation model data



We realize that for the three cases, the production of oil, gas and water varies with respect to time and the data issued from the simulation does not reflect reality which is data gotten from production history. We will therefore create a model that will be closer to the real model by doing a history match.

- Simulation data versus historical data based on pressure.

Fig.13 presents the evolution of the average reservoir pressure on the x-axis (Ave Pres POVO SCTR) with respect to time (y-axis) for the two models. The curve in red represents simulation data (reservoir.irf) and historical data is represented in blue viewed as round circles (RESERVOIR-PRESSURE-HISTORY.fnf). We observe that, for the simulation model (red curve):

- From the first day (2000) the average pressure which is 20758 kPa decreases progressively up to 16984 kPa in 2005-01-01.
- From 2005 up to the end of production, the average pressure decreases slightly from 16984 kPa and 14148 kPa.

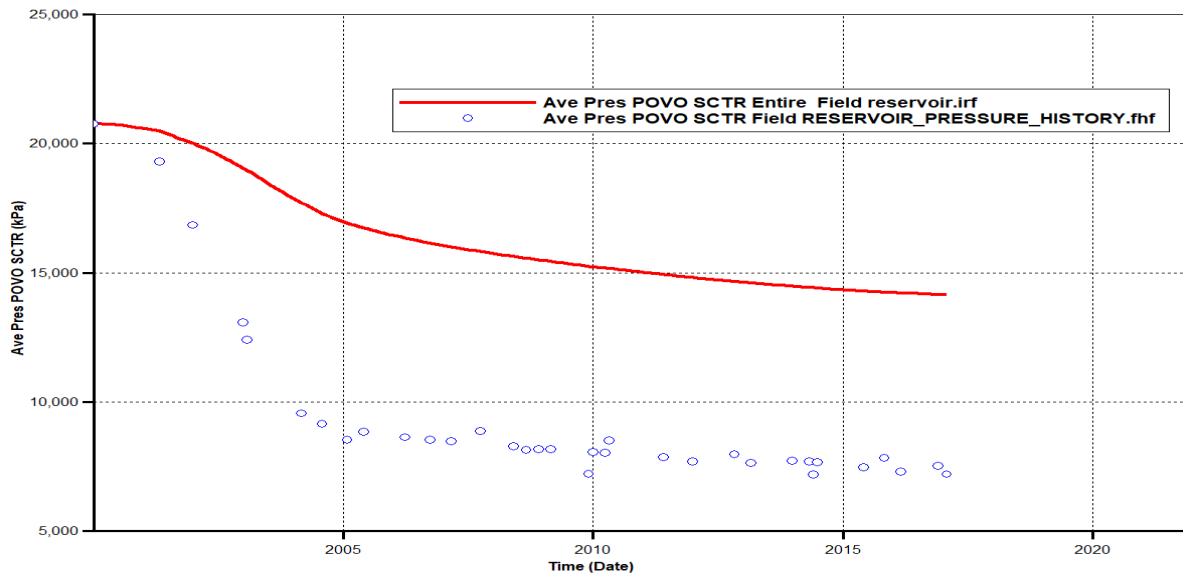
For the model issued from historical data that is the blue curve varies as such:

- From the first day (2000) the average pressure which is 20758 KPa decreases rapidly up to 8534 kPa in 2005-01-01.

- From 2005 up to the end of production, the average pressure decreases slightly from 8534 kPa and 7196 kPa.

We observe here that for the case of average reservoir pressure; **simulation data (reservoir.irf)** and **historical data (RESERVOIR-PRESSURE-HISTORY.fnf)** are not superposed as a result we will do an approach based on the historical matching model to ameliorate the final model.

Figure 13: Average pressure of reservoir based on historical and simulation model data



Scenario 2: History matching

The knowledge of historical data and their superposition is the initial step to know the behavior of the reservoir, the differentiability of the wells and the identification of a better model for the prediction. Therefore, it is based on the calculation of historical data by the software and that coming from the field.

• Historical Matching for Production and Pressure

The data from the Lokele field, which is subject of our study, are raw data that have not undergone any processing, this is why it must be explored and processed by a match and identify the best parameters in order to better improve our production.

The choice of a best prediction model goes through a dataset (match) based on the change of parameters that have an important impact in the reservoir. For example, the rock compressibility and the relative permeability. This technique requires several iteration times of values for the choice of the best model.

Changing rock compressibility to match production and pressure behavior.

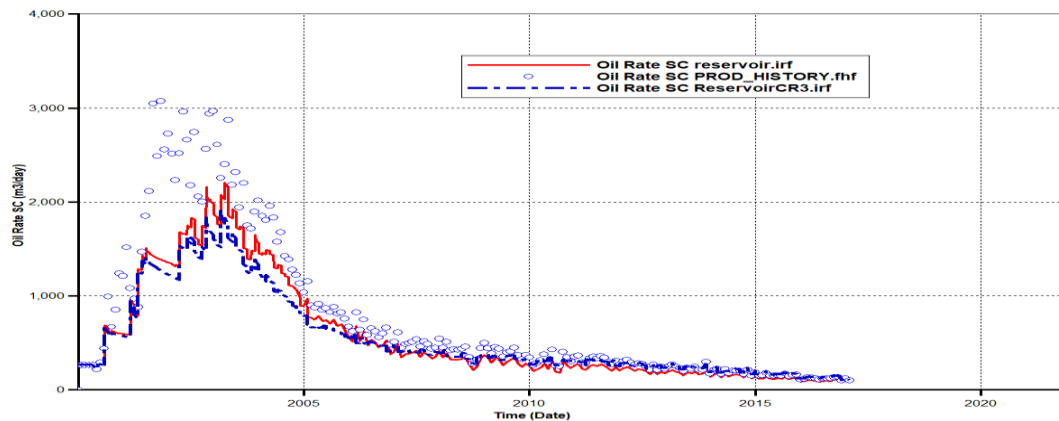
a) Production

After several possible iterations of the rock compressibility values, the best value taken is $0.001e-06$ 1/KPa. Fig.14 presents the impact of the modification of the best rock compressibility values for oil production. For the case of the impact of this rock compressibility of gas and water production, we would present it in appendices 2. We can thus visualize the evolution of oil production (Oil Rate SC (m3)) on the y-axis as a function of time on the x-axis. We notice that;

Between 2000 and 2005 the production history data based on the field (Oil Rate SC PROD_HISTORY.fnf) shown as blue round circles, that are based on the calculation done by CMG simulator in red (Oil Rate SC reservoir.irf) and that based on the same calculation done by the simulator for change in rock compressibility values; curve in thick blue color (Oil Rate

SC ReservoirCR3.irf) do not superpose well, but between 2005 to 2017 these three models tend to superpose well. The choice of a good superposition will better impact production.

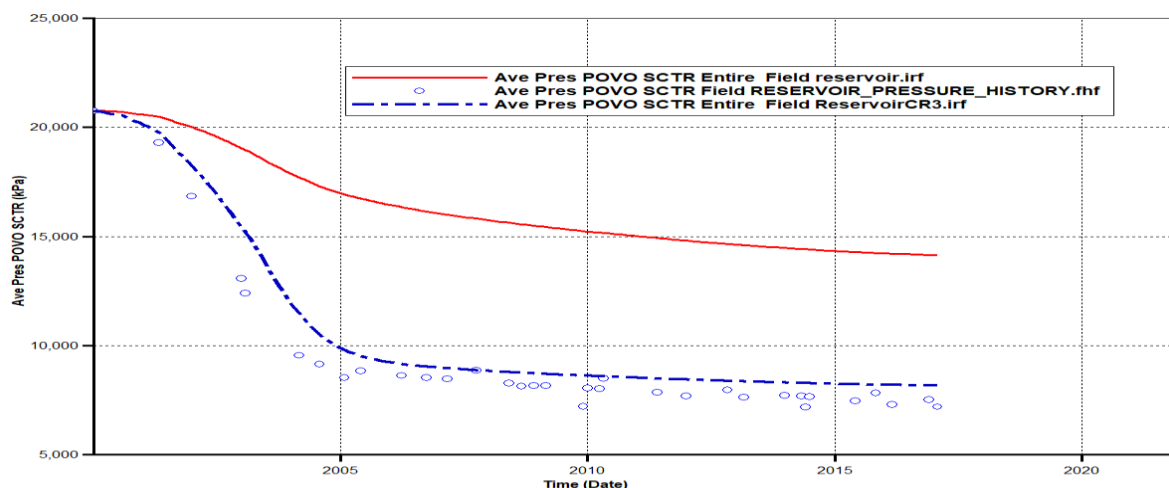
Figure 14: Matching for rock compressibility value equals to 0.001e-06 1/KPa.



b) Pressure

Fig.15 still follows the same iteration process in choosing the best model of change in rock compressibility values. Here for the case of pressure, the value recovered is 0.001e-06 1/KPa and we see from the figure that the model coming from the best rock compressibility in blue broken lines (Ave Pres POVO SCTR Entire fieldReservoirCR3.irf) is closer to the model based on production history also in blue lines but with circles (Ave Pres POVO SCTR Field RESERVOIR_PRESSURE_HISTORY.fhf) but it is very distant from the model resulting from the CMG simulator (curve in red: Ave Pres POVO SCTR Entire field reservoir.irf) model. So as the two models in blue are not well superposed; to better improve, we will further modify the second parameter which is the relative permeability.

Figure 15: Reservoir pressure behavior for the best model

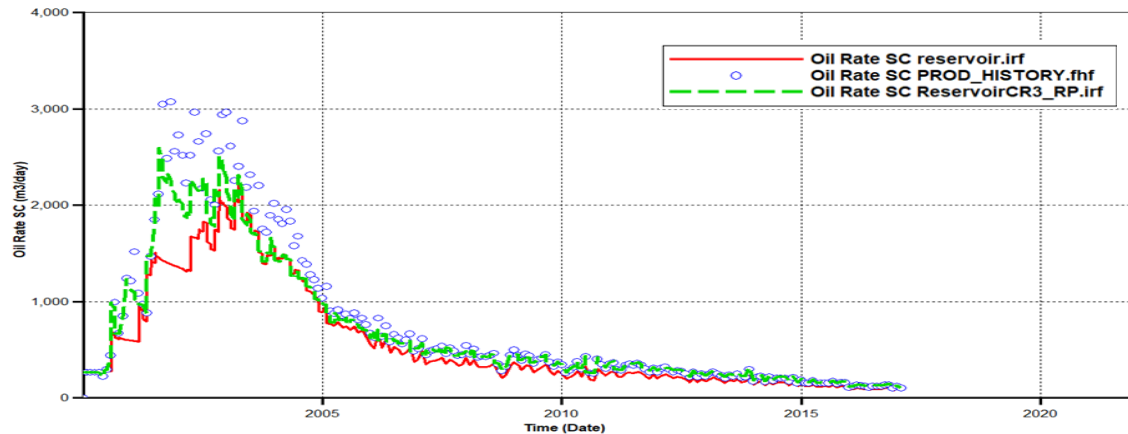


Changing relative permeability Curves to match production

The amelioration of the model Oil Rate Reservoir SC ReservoirCR3.irf will be based on the modifications of the relative permeabilities of the reservoir. Fig.16 below represents the evolution of the oil flowrate with respect to time. The curves are based on the three models; the red curve represents the initial simulation model (Oil Rate SC reservoir. irf), the blue curve with bubbles (Oil Rate SC PROD-HISTORY.fnf), and the green curve with broken lines (Oil Rate ReservoirCR3-RP.irf) is the model issued from the Fig.IV.12 where we were able to find the best value for relative permeability by bringing the model in green color closer to the model in blue color. So, the best values are: KROCW (Relative permeability of oil at connate water)

=0.4 and KROGCG (Relative permeability of oil at connate gas) =0.4. We observe that for the three possible configurations there is a superposition of curves, despite the slight fluctuation between 2000 and 2009. For the case of water and gas we would see it in the appendices 3. The choice of a best model results from the simulation of reservoir parameters that impact pressure and production, as such the model used to do predictions will be that in which the relative permeability of the reservoir was modified (Oil Rate ReservoirCR3-RP.irf). This will therefore lead to an improvement in the production rates.

Figure 16: Matching for relative permeabilities equals 0.4



Scenario 3: Prediction

Base case model

Base case model is a prediction using the best matching model through the steps of identifying the last pressure values issued from historical bottom hole pressure data from the simulation of the best model and thereby forecasting it to a future date.

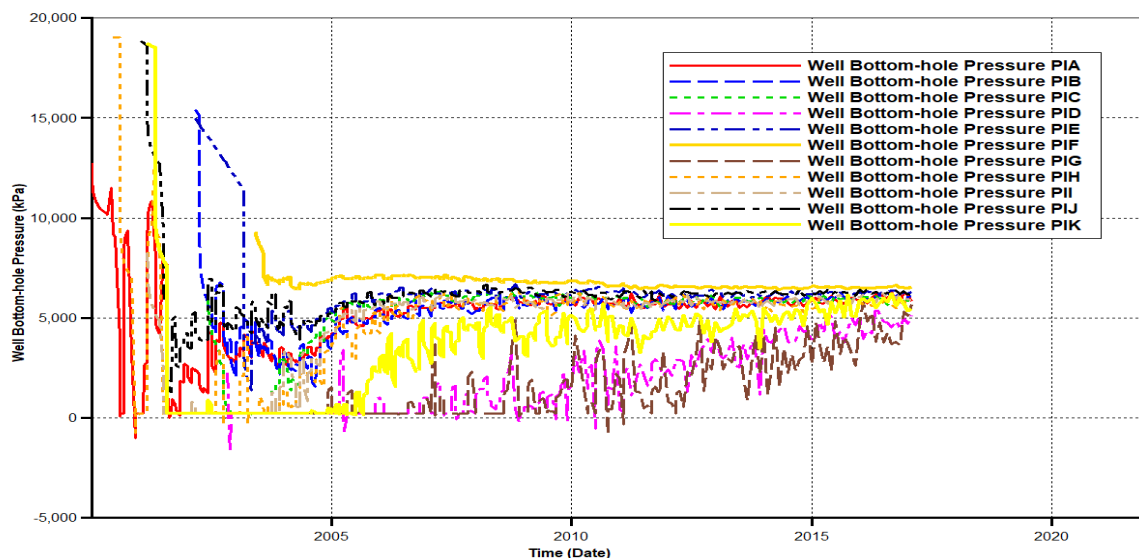
- **Evaluating best values for Bottom Hole Pressures in all the wells.**

Fig.17 presents the variation of the BHP of the 11 wells with respect to time.

- From 2000 to 2005 the pressure in each well runs from about 19,000kPa to about 6000kPa so it drops progressively.
- From 2005 to 2017 this pressure is in the interval of 0 and 6000kPa.

Thus, Fig.17 will permit us to identify the last pressure values (2017) and assign it to Tab.5 for an initial prediction based on the change of Bottom Hole Pressure (BHP) values.

Figure 17: BHP behavior for all the 11wells



Tab. 5 permits to identify the last BHP values in each well with the aim of injecting it as the start value for the prevision of the base case model.

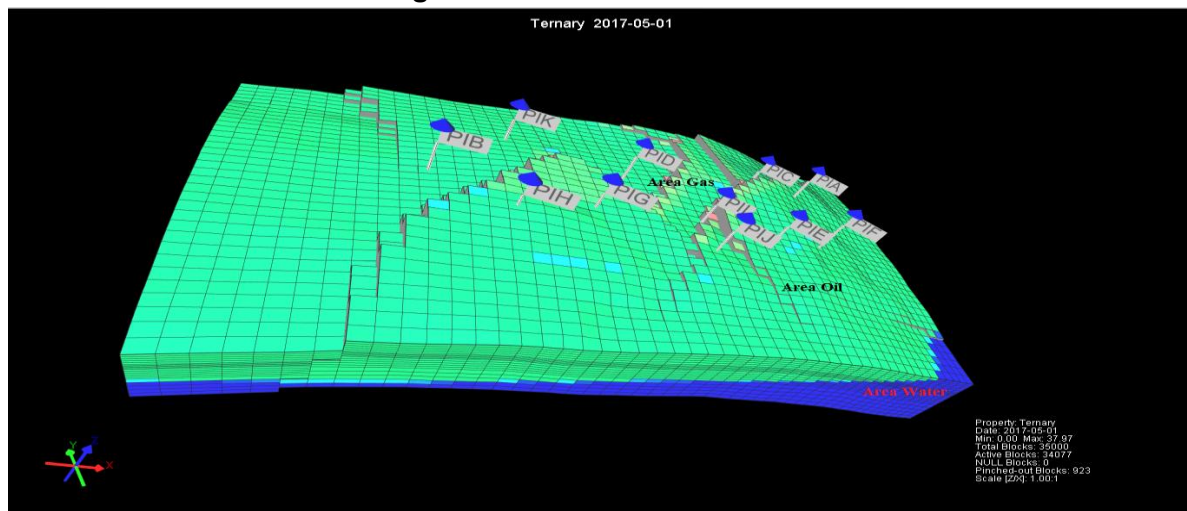
Table 05: Last BHP values for all wells

Well	PIA	PIB	PIC	PID	PIE	PIF	PIG	PIH	PII	PIJ	PIK
Date	2017	2017	2017	2017	2017	2017	2017	2017	2017	2017	2017
BHP(Kpa)	5806.4	6085.9	5988.6	5151.6	6313.9	6542.0	5664.5	5802.7	5896.4	6139.5	5464.3

- **Base case Prediction.**

The 3D grid ternary model in Fig.18 gives us an overview of the fluid contact present in our reservoir with the green color illustrating the oil zone, the grey color illustrating the gas zone and the blue color illustrating the water zone and the positioning of the 11 production wells used to recover pressure values just before prediction (2017).

Figure 18: 3D Base case model



After visualizing the 3D reservoir model, the behavior of the wells in the reservoir can be further known during the historical and prediction phase of the base case model built from the best model taken during matching.

Fig.19 shows the evolution of oil and recovery factor curve with respect to time. The curve in blue (Oil Rate SC Default-Field-PRO) represents the model of oil rate that is the oil volume produced after simulation, as such the data is based on production history and that simulated by the machine. The curve in green with broken lines (Oil Recovery Factor SCTR Entire Field) represents the oil recovery factor after the simulation of the base case model.

We notice here that:

- From 2000 to 2017 which represents the production history period, the curve in blue (Oil Rate SC Default-Field-PRO), there is a progressive decrease in the quantity of oil produced per day due to the depletion of the reservoir caused by the absence of a good drainage mechanism (the aquifer does not occupy the water zone). This depletion is more accentuated in 2016 the year in which hydrocarbon recovery becomes impossible. The recovery factor (green curve) runs from 0 to 10.37.
- From 2017 to 2030 (prediction period) the blue curve almost tends to remains constant with value between $127.15m^3/day$ and $52.58m^3/day$. During this period the recovery factor slowly increases, from 10.37 to 11.24. This makes the recovery factor of the base case model to be approximately 55 percent.

We realize that for both curves in the case of production history, when there's variation in production the oil recovery factor increases progressively and when this variation is no longer observed in the prevision phase, the recovery factor tends to be constant. This shows the impact of pressure on production prediction.

Figure 19: Curve of Oil rate and Oil recovery factor with respect to time

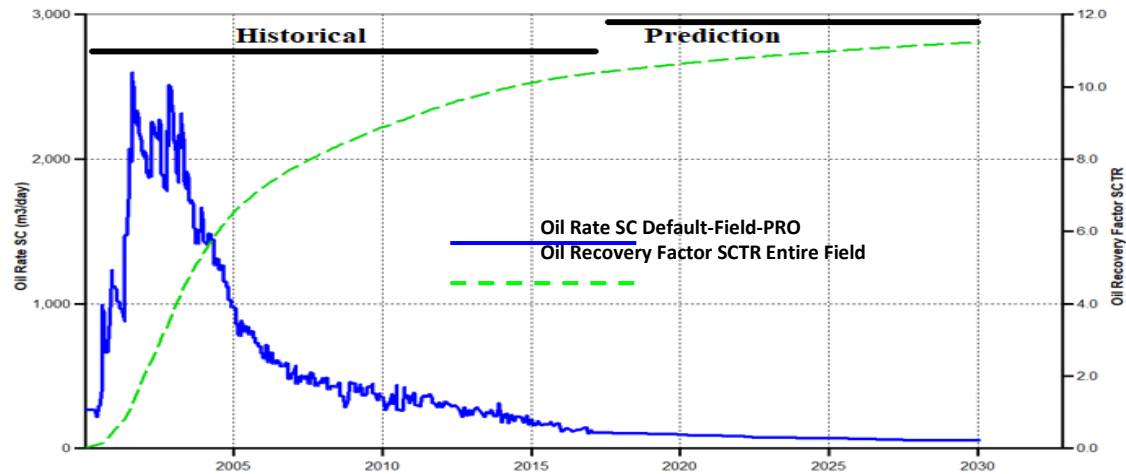


Fig.20 shows the evolution of gas and recovery factor curve with respect to time. The curve in blue (Gas Rate SC Default-Field-PRO) represents the model of gas rate after simulation with data based on production history and that simulated by the machine. The curve in green (Gas Recovery Factor SCTR Entire Field) represents the gas recovery factor after the simulation.

We remark that:

- From 2000 to 2017 the curve in blue (Gas Rate SC Default-Field-PRO) represents the production history period and when it varies the recovery factor (green curve) runs from 0 to 10.022.
- From 2017 to 2030 (prediction period) the blue curve tends to remains constant with value between $4073.26m^3/day$ and $3270.09m^3/day$. During this period the recovery factor slowly increases, from 10.022 to 11.29.

We realize that for both curves in the case of production history, when there's variation in production the gas recovery factory increases progressively and when this variation is no longer observed in the prevision phase, the recovery factor tends to be constant.

Figure 20: Curve of Gas rate and Gas recovery factor with respect to time

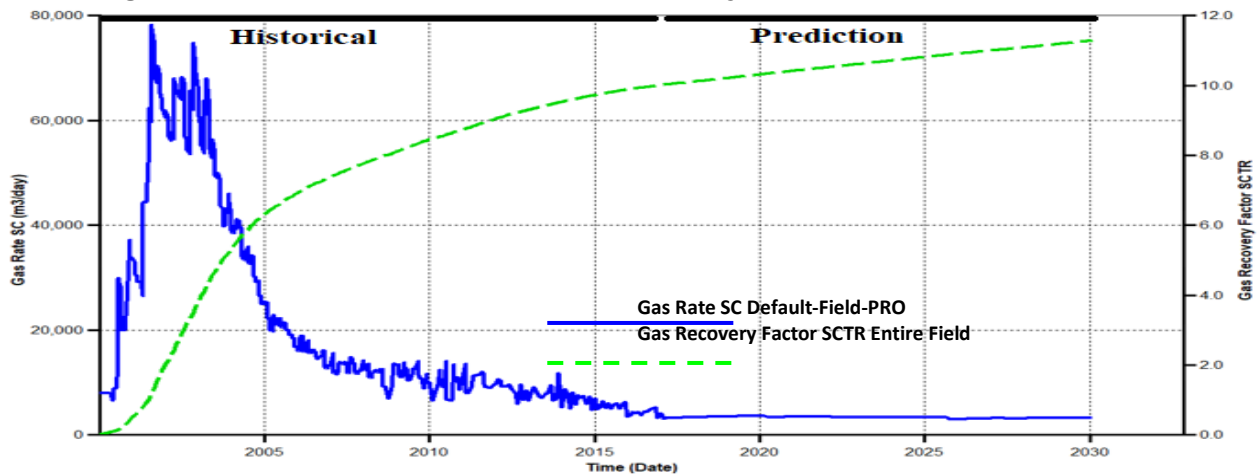
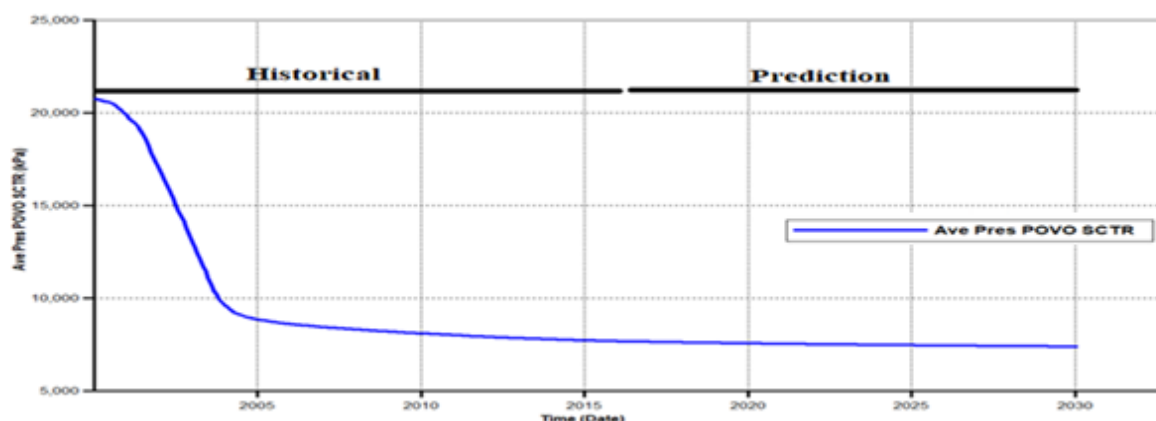


Fig.21 shows the evolution of average pressure in the reservoir (Ave Pres POVO SCTR) with respect to time. It varies as such:

- From 2000 to 2004 the pressure decreases progressively from 20798.4kPa to 9305.86kPa, due to increase in production.
- From 2004 to 2030 the pressure leaves from 9305.86kPa to 7388. 56kPa and tends to remain constant. This is due to the absence of a sufficient drainage mechanism to maintain pressure in the reservoir decreasing production of hydrocarbons.

Figure 21: Curve of average reservoir pressure with respect to time



Predictions based on the change of BHP values in the based case model showed us a prediction that did not ameliorate our production so the base case model is not enough to optimize production. All this just permits us to know if the production went on well and in the second case (CO₂ injection) we will ameliorate this situation.

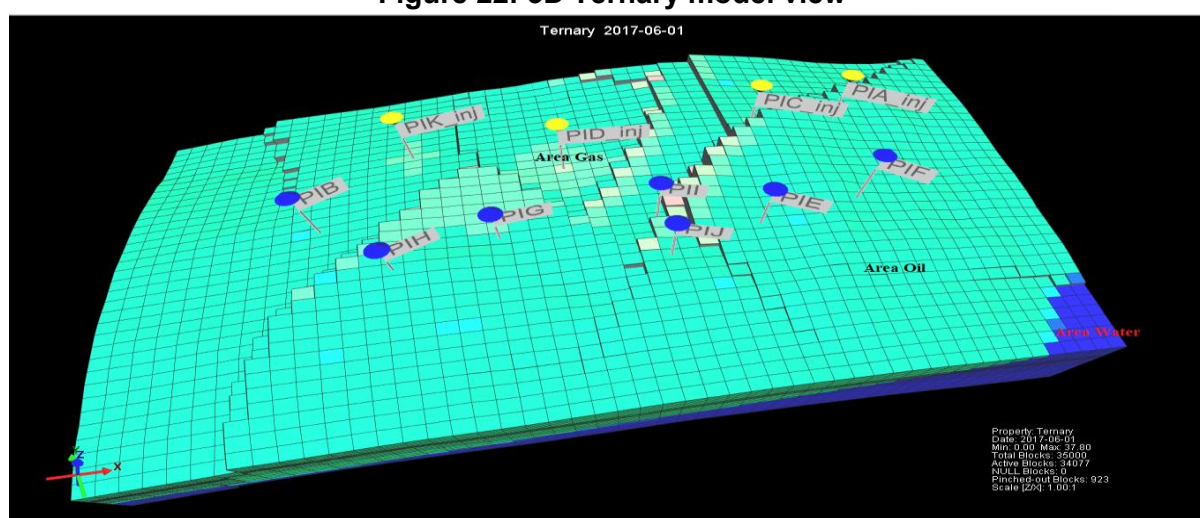
CO₂ injection model

From the base case model, the next steps will allow us to use the CO₂ stored and that coming from the atmosphere to improve production of our field, so we will initially identify production wells closed to the gas zone, and transform them into injection wells the CO₂ injection fluid while introducing the injected flowrate. For this we have to make:

- **A Choice of the injection wells**

The choice of the transformation of the production wells is based on the identification of the gas zone. With respect to this, the wells closed to this zone, which are four in number, have been transformed into injection wells as shown in Fig.22 described by the ternary model where we observe the gas zone in gray color, the oil zone in green color and the water zone in blue color. Therefore, we see that the wells transformed to injection wells are PIK_inj, PID_inj, PIC_inj, PIA_inj (the wellheads in yellow). The other 7 wells will undergo an improvement in production due to the action of the injection wells.

Figure 22: 3D Ternary model view



- **Injection of 1,600,000m³ of CO₂**

Fig.23 shows the evolution of oil rate, recovery factor and gas rate injection curves with respect to time. The curve in blue (Oil Rate SC Default-Field-PRO) represents the model of oil rate after simulation, as such the data is based on production history and that simulated by the

machine. The curve in green (Oil Recovery Factor SCTR Entire Field) represents the oil recovery factor after the simulation and the red (Gas Rate SC Default-Field-INJ) represents the gas rate injected during prediction. We observe two phases:

- **Historical Phase**

The historical period within 2000 to 2017, injection was not performed so the flowrate is null. This is materialized by the red line curve that touches the x-axis. Thus, we observe the same variation of oil rate in blue and the oil recovery factor in green. As a result of no injection, we have no amelioration of oil production.

- **Prediction Phase**

The prediction period from 2017 to 2030, for a CO₂ rate injected of 1.600.0000m³, we observe an increase in oil production between 2017 and 2018 from 51m³/day, to 1388.08m³/day. During this same time, the recovery factor increases from 50 percent to 55 percent, this is due to the start of CO₂ injection. Between 2018 and 2030 the maximum injection rate (1,600,0000m³) reached its limit and remained constant, this caused a gradual drop in oil production (curve in blue color) which went from 1388m³/day to 132m³/day. At the same time, the recovery factor curve continues to increase from 55 percent to 75 percent. The increase observed in the pressure flowrate of oil at the beginning of injection is due to the fact that CO₂ is an expandable gas and will therefore expand progressively to sweep oil to the production well thus the injection of CO₂ has significantly improved the production of oil. The decrease in the pressure flowrate of oil is due to the fact that the quantity of gas stored becomes insufficient to maintain a constant pressure. Meanwhile, the recovery factor keeps increasing cause the oil produced does not impact production but it is influenced by injection.

Figure 23: Impact of CO₂ injection in Oil Recovery

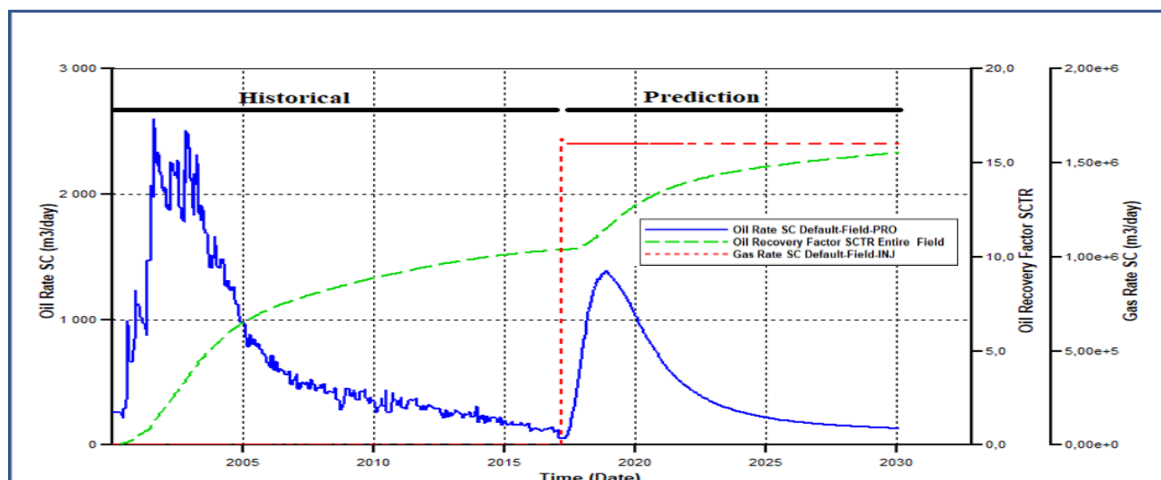


Fig. 24 represents the effect of CO₂ injection on gas production with respect to time. The curve in green (Gas Rate SC Default-Field-PRO) represents the model of oil rate after simulation with data based on production history and that simulated by the machine and the red curve (Gas Rate SC Default-Field-INJ) represents the gas rate injected during prediction. We observe two phases:

- **Historical Phase**

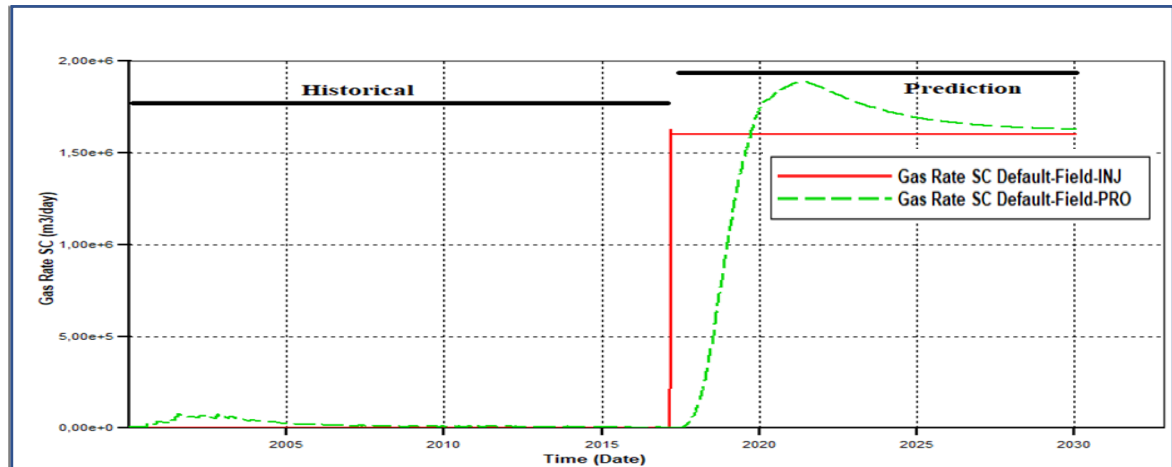
The historical period within 2000 to 2017, injection was not performed so the flowrate is null, materialized by the red curve that touches the x-axis. Thus, we observe the same variation of gas rate in green. As a result of no injection there is no amelioration of gas production.

- **Prediction Phase**

For an injection of 1,600,000m³(red curve) of gas we observe between 2017 and 2021 a gross increase in the gas flowrate (curve in green color) from 0 to 1,886,700m³/day. From 2021 to

2030 there is a slight drop in the gas flowrate as seen on the green curve from 1,886,600m³/day to 1,628,190m³/day. This increase in the gas flowrate after injection of CO₂ is due to the fact that we produce and inject CO₂ at the same time. This turns to confirm what we saw in Fig.IV.20 of the 3D grid a small gas zone implying our reservoir is very rich in oil hence the black oil model.

Figure 24: Impact of CO2 injection in Gas Production



During CO₂ injection, to produce more hydrocarbons, a good control of surface pressure is required. So, Fig.25 represents pressure behavior within the two phases, materialized in red color (Ave Pres POVO SCTR).

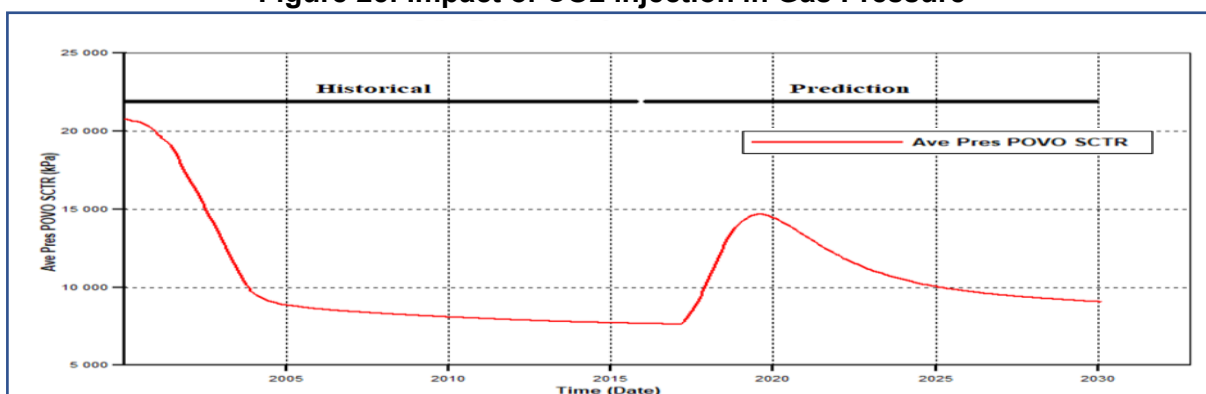
- **The Historical Phase.**

From the historical period between 2000 to 2017, we observe a variation in reservoir pressure analyzed in figure 25.

- **The Prediction Phase**

We observe from 2017 to 2019 an increase in pressure from 7642kPa to 14675kPa, thus during this period the injected flowrate required an increase in pressure of the injection well. From 2019 to 2030 this pressure dropped progressively to 9693kPa this is due to the gradual decrease in predicted production.

Figure 25: Impact of CO2 injection in Gas Pressure



The Tab.6 presents the record of the cumulative oil production, gas and recovery factor produced during the end of historical and prediction phase. We see that after injection, oil volume, gas volume and recovery factor have been improved.

Table 06: Cumulative Production for the two phases

Phase	Date	Cumulative oil (m ³)	Cumulative gas (m ³)	Oil Recovery Factor
Historical	2017	4,292,080	124,980,000	50 percent
Prediction	2030	6,418,570	7,184,650,000	75 percent

Economic Evaluation

This paper on techno-economic analysis provides the fiscal precursor and its outlook for Iokele field for CO₂-EOR implementation starting from the year 2016 with a projection of 14 years project lifetime. The calculation outputs of project cash flow and total annual cash outflows, as well as its inflows throughout its lifetime, is as shown in Figure 26.

Figure 26: Project cash flow

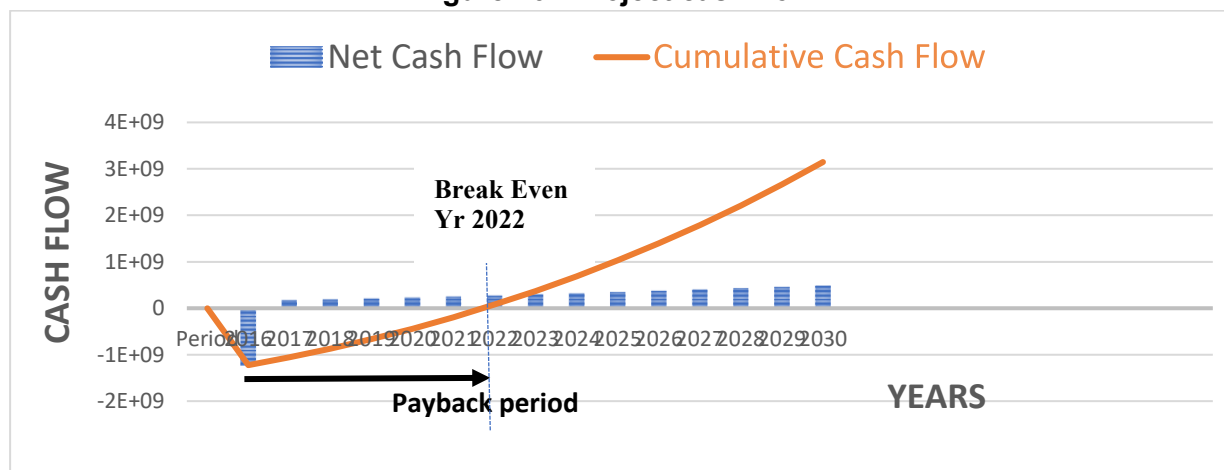


Table 07: Economic Results

Parameters	Results
Capital cost (USD Millions)	887.9
O&M cost including abandonment cost (USD Millions)	306.3
Payback Period (PBP)	5.54 Years
Net Present Value (NPV)	1445.0
Internal Rate of Return (IRR)	25.69 percent

For a CO₂-EOR project to be considered techno-economically viable, it has to archive the 3 decision variables of an NPV>0, followed by an IRR value higher than the specified discount rate along with PBP being lower than the field production lifetime. So, we can conclude that our economic results as seen on the table above show that our project is economically viable and thus can be effectively implemented on the Iokele field.

Sensitivity Analysis (SA) Results and Discussion

Sensitivity Analysis (SA) evaluates and pinpoints the key variables affecting CO₂-EOR project performance by examining the effect of input variable modification on the model's outcome. By identifying their range of elasticity and evaluating the impact of the variable's favorable or unfavorable perspective on project performance in a variety of scenarios. Variation scenarios and their effects on the three input variables—oil and gas price (cash inflow), discount rate, and capital cost—as well as their effect on the risks affecting the fiscal precursor, net present value (NPV), and its sensitivity range, are shown in Figures 27 to 29.

Figure 27: Sensitivity analysis (SA) of Net Present Value (NPV) with Price Variation

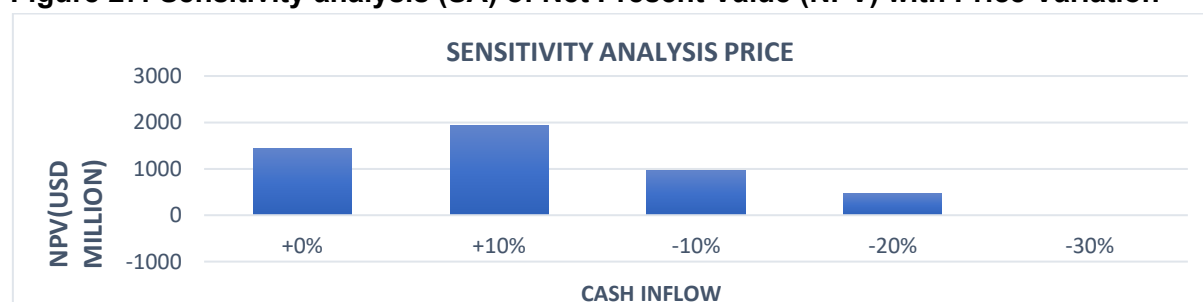


Figure 28: Sensitivity analysis (SA) of Net Present Value (NPV) with Discount percent

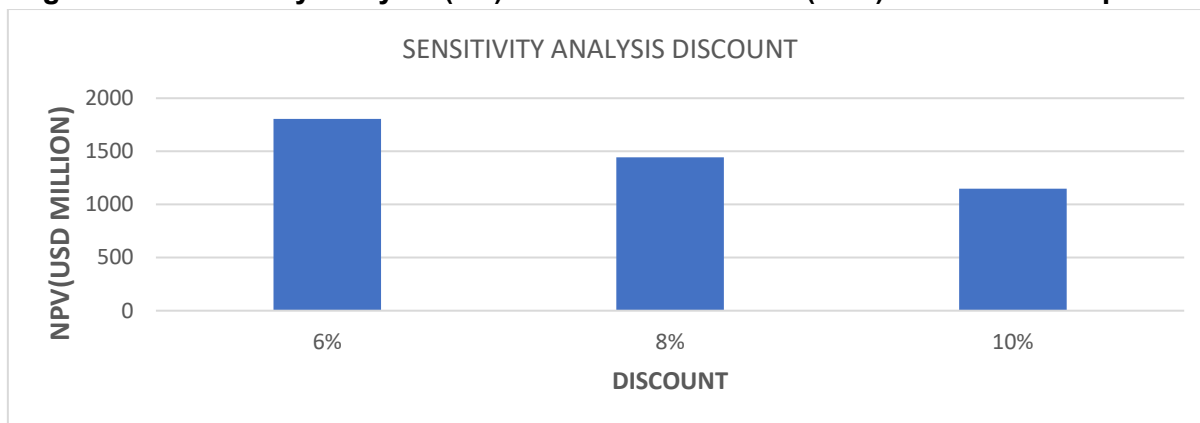
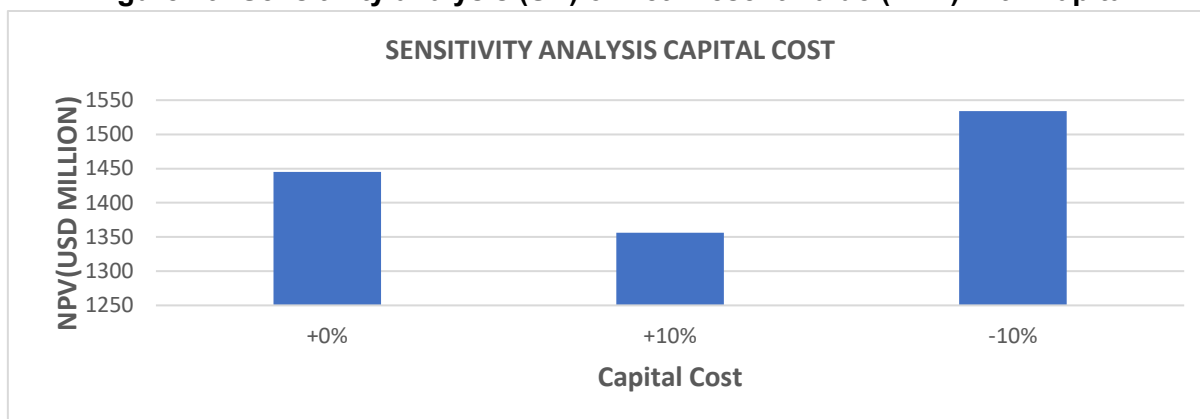


Figure 29: Sensitivity analysis (SA) of Net Present Value (NPV) with Capital



In comparison to the other variables, cash inflow (gas price and oil prices) demonstrates the most substantial NPV impact change. The output from discount rate, capital cost (from the most affecting) variables are found to less influencing as compared to cash inflow (gas price and oil prices). In figure 4a when when gas and oil prices increase it increases the NPV and when it decreases it affects the NPV negatively as we notice that at a 30 percent decrease in price we have a negative NPV of -12 (USD millions). In the other case of discount rate, an increase of 10 percent per annum results to and decrease in NPV to 1148.4 (USD millions) whereas a decrease to 6 percent per annum will result to an increase in NPV to 1806.4 (USD millions). When the Capital cost is increased to 10 percent it results to a decrease in the NPV to 1356.2 (USD millions) mean while a decrease in capital cost of 10 percent when increase the NPV to 1533.8 (USD millions).

Conclusion and Perspective

This paper has presented a comprehensive techno-economic analysis of CO₂-EOR of depleted reservoirs, with a focus on its application in the Lokele Field in Cameroon. The study has shown that CO₂-EOR is a technically feasible and potentially profitable method for enhancing oil recovery in the Lokele Field, with the potential to increase the recovery factor by up to 25 percent. The economic analysis has demonstrated that the project has a positive net present value (NPV) of 1445 (USD million), a payback period (PBP) of 5.54 years, and an internal rate of return (IRR) of 25.69 percent. However, the analysis has also revealed that the viability of the project is highly sensitive to key factors such as the CO₂ capture cost and capital cost, the oil and gas price, and the discount rate.

The study has contributed to the understanding of the technical and economic factors that affect the viability of CO₂-EOR in depleted reservoirs, and has highlighted the need for careful consideration and management of these factors in the planning and implementation of

CO₂-EOR projects. The study has also identified several areas for further research and field testing, including the validation of the simulation models and assumptions used in the analysis, and the investigation of the potential environmental impacts of CO₂-EOR. Overall, the study has shown that CO₂-EOR can be a viable and attractive option for enhancing oil recovery in depleted reservoirs, including in the Lokele Field. However, its success depends on a range of technical, economic, and regulatory factors that need to be carefully considered and managed. The findings of this study can be used as a basis for further research and development of CO₂-EOR projects in Cameroon and other regions.

References

1. <https://unfccc.int/news/global-co2-emissions-rebounded-to-their-highest-level-in-history- in-2021>.
2. Daniel P. Arnold, Multi-objective optimization of CO₂ recycling operations for CCUS in presalt carbonate reservoirs, September 2022.
3. Jessen, K. Kovscek and Orr, F. Increasing CO₂ Storage in Oil Recovery, Energy Conversion Management, Page 293-311, 2005.
4. Lei Zhang, Optimization based approach for CO₂ utilization in CCUS supply chain, April 2020.
5. Jikich, S. A., Smith, D. H. Sam, W. N. and Bromhal, G. S, Enhanced Gas Recovery (EGR) with Carbon Dioxide Sequestration: A Simulation Study of Effects of Injection Strategy and Operational Parameters; Regional/AAPG Eastern Section Joint Meeting held in Pittsburgh, Pennsylvania; SPE 84813, Proceedings of the SPE Eastern.
6. <https://www.businessincameroon.com/public-management/2709-12770-iss-africa-sees-cameroon-s-carbon-emissions-at-15-1-mln-tons-by-2043>, consulted 10/10/2022.
7. Contribution déterminée au Niveau National (CDN) NATIONALLY Determined Contribution-Actualized Updated (NDC), Emergent Cameroon, September 2021, Page 2 and Page 49
8. <https://eitcameroon.org/post/253>, consulted 17/10/2022
9. Wang J, Wang Z, Ryan D, Lan C; A study of the effect of impurities on CO₂ storage capacity in geological formations.; Green Gas Control 2015; Page 132–7.
10. Ansari Zadeh, M, Dodds, K, Gurbinar, O., Pekot, L. J, Kalfa, Sahin, S., Uysal, S., Ramakrishnan, T. S., Sacuta, N., & Whittaker, Carbon dioxide challenges and opportunities, (2015). In Oilfield Review (Vol. 27), Page 25-43.
11. Bouzalakos, S.; Overview of carbon dioxide (CO₂) capture and storage technology. Developments and Innovation in Carbon Dioxide (CO₂) Capture and Storage Technology, (2010). Page 1–24.
12. <https://www.ipcc.ch/report/ar5/syr/>, consulted on the 17/9/2022.
13. Butler, J.N., Carbon dioxide equilibria and their applications. Routledge, 2019.
14. June Sekera, Andreas Lichtenberger; Carbon Dioxide Enhanced Oil Recovery (CO₂ EOR): Factors Involved in Adding Carbon Capture, Utilization and Storage (CCUS) to Enhanced Oil Recovery, 2012.
15. Insights Series. IEA, Storing CO₂ through Enhanced Oil Recovery. (2015), Page 45-67.
16. <https://afrimag.net/societes/african-energy-chamber/>, consulted 17/10/2022.
17. Figueroa, Int. J. Green. Advances in CO₂ capture technology-The US department of energy and carbon sequestration program, Gas Control 2008, 2, Page 9–20.
18. TZETE, Nathalie¹ DJIBIE, Lionel NFOR, Julius TSALEFAC Maurice. Impacts de la consommation des ressources en énergies fossile dans les activités, d'exploitation des carrières industrielles de l'Ouest CAMEROUN, Université de DSCHANG Page 5.
19. SIE-Cameroun, "Situation Energétique du Cameroun : Rap- port 2011," Ministère de L'eau et de L'énergie, Yaoundé, 2012, Page 45.
20. <https://www.hysacam-proprete.com>, accessed 14/08/2022.
21. <https://web.facebook.com/photo/?fbid=708713060471861&set=pcb.708713213805179>, accessed 2022.
22. Joginder Singh and Praveen Gehlot, Microbial Carbon Sequestration, 14 Publisher Agrobios (India) Editors, April 2016, Page 227-241.
23. Terrestrial sequestration of carbon dioxide (CO₂). Developments and Innovation in Carbon Dioxide (CO₂) Capture and Storage Technology, Lal, R. (2010), Page 271–303.
24. <https://inhabitat.com/masdar-and-oil-companies-to-develop-worlds-first-commercial-scale-carbon-capture-storage-project>, accessed 22/08/2022.
25. Kambale, J, & Tripathi, V. (2010). Biotic and abiotic processes as a carbon sequestration strategy. In Journal of Environmental Research and Development (Vol. 5).
26. https://en.wikipedia.org/wiki/Carbon_storage_in_the_North_Sea, accessed 14/07/2022.
27. Metz, B., Davidson, O., de Coninck, H., Loos, M., & Meyer, L., Carbon Dioxide Capture and Storage, (2005).
28. Bachu, Maroto-Valer (Ed.), Characterization techniques for the geological sequestration of carbon dioxide (CO₂), Wood head Publishing Series in Energy Vol. 2, Page 27–56.
29. International Energy Agency (IEA), CO₂ Capture and Storage in Geological Formations, 2002.
30. <https://www.ipcc.ch/report/carbon-dioxide-capture-and-storage>, consulter 17-02-2022.

31. Hendriks, C.A. and Block, Underground Storage of Carbon Dioxide, K.; Energy Conversion and Management; Volume 34, 1993.
32. Franklin, M. and Orr, Jr.; Storage of Carbon Dioxide in Geologic Formations; Distinguished Author Series; September 2004.
33. Krumhansl, J.L., Stauffer, P. H., Lichtner, P. C., And Warpinski, Geological Sequestration of CO₂ in a Depleted Oil Reservoir; N. R.; paper SPE 75256, presented at the SPE/DOE Improved Oil Recovery Symposium, Tulsa, Oklahoma, USA, Page 13-17 April 2002.
34. Wang Z, Wang J, Lan C, Ryan D, et al.; A study on the impact of SO₂ on CO₂ injectivity for CO₂ storage in a Canadian saline aquifer; Energy 2016; Page 184.
35. CO₂ Injection & storage 2015. <http://old.co2crc.com.au/aboutccs/storage>, accessed May 16, 2017.
36. <https://www.bing.com/imaFCartoon-plot-depicting-CO2-trapping-mechanisms-and-their-effective-carbon-dioxide-trapping-mechanisms>, consult 22/05/2022.
37. L. Zhang, S. Ren, B. Ren, W. Zhang, Q. Guo, and L. Zhang; Assessment of CO₂ storage capacity in oil reservoirs associated with large lateral/underlying aquifers: case studies from China; International Journal of Greenhouse Gas Control, vol. 5, Page 1016- 1021, 2011.
38. A. Chadwick, R. Arts, C. Bernstone, F. May, S. Thibeau, and P. Zweigel; Best practice for the storage of CO₂ in saline aquifers, British Geological Survey Occasional Publication, vol. 14, Page 267, 2008.
39. <https://www.google.com/search?q=enhanced+oil+recovery+flow+chart&client=firefox-accessed> 2022.
40. T. E, G. A, G. C. C and P. S. D, European Commission Joint Research Center.
41. Enhanced Oil Recovery using Carbon Dioxide in the European Energy System;
42. Kinjal Partel, M.N. Mehta, Twinkle Patel the Power Series Solution of Fingering Phenomenon Arising in Fluid Flow through Homogenous Porous Media. January 2011
43. <https://www.google.com/search?q=enhanced+oil+recovery+flow+chart&client=firefox-b-accessed> 2022.
44. <https://www.google.com/search?q=enhanced+oil+recovery+flow+chart&client=firefox-b-accessed> 2022.
45. [http://www.CO₂ storage solutions.com/index.html](http://www.CO2-storage-solutions.com/index.html), accessed May 16, 2022.
46. Tzimas et al. Enhanced Oil Recovery using Carbon Dioxide in the European Energy System, (2005), Page 465-555.
47. <https://www.energy.gov/fecm/science-innovation/oil-gas-research/enhanced-oil-recovery>, accessed 2022.
48. <https://www.sciencedirect.com/topics/engineering/original-oil-in-place>, accessed 04/10/ 2022.
49. <https://link.springer.com/book/10.1007/978-3-319-55843-1>, accessed 02/10/ 2022.
50. Bui M, Gunawan I, Verheyen V et al (2014) Dynamic modelling and optimisation of flexible operation in post-combustion CO₂ capture plants-A review. Computer Chem Eng 61:245–265
51. Computer Modeling Group (CMG) Ltd., <http://www.cmggroup.com>, August 2005.
52. Tool CMG, 2015, Page 12-34.
53. Katie Lebling, Haley Leslie-Bole, Zach Byrum and Liz Bridgwater; Things to Know About Direct Air Capture; By Publishing May 2, 2022, Page 33-34.
54. Biomass with CO₂ Capture and Storage (Bio-CCS), European Technology Platform for Zero Emission Fossil Fuel Power Plants, Page 32.
55. <https://ocean-climate.org/en/awareness/the-ocean-a-carbon-sink>, accessed 12/05/2022.
56. Olabi, A.G; Abdel Kareem, M.A; Renew. Sustain. Assessment of the pre-combustion carbon capture contribution into sustainable development goals SDGs using novel indicator Energy Rev. 2022, Page 153
57. [56] Rubin, E. S., Mantripragada, H., Marks, A., Versteeg, P., & Kitchin, J, Progress in Energy and Combustion Science, (2012). The outlook for improved carbon capture technology; (2012). Page 630
58. Carbon Dioxide Sequestration and Enhanced Oil Recovery Co-Optimization, Nuri akhundov, thesis submitted to the graduate school of natural and applied sciences of middle east technical university, master of science in petroleum and natural gas engineering, September 2021, page 36-38.
59. Thorin Daniel; Alice Masini; Cameron Milne Neeka; Nourshagh Cameron; Iranpour JinXuan, Techno-economic Analysis of Direct Air Carbon Capture with CO₂ Utilization Carbon Capture Science & Technology Volume 2, March 2022, Page 4-5.
60. Maung Phyo Wai Aung; Analysis on EOR/CO₂ Sequestration in Sacroc Unit, Texas Using a Compositional Simulator; THESIS Faculty of Petroleum Engineering Department New Mexico Institute of Mining and Technology; Page 12-16.
61. Aibar Kamashev and Yerlan; Amanbek, Reservoir Simulation of CO₂ Storage Using Compositional Flow Model for Geological Formations in Frio Field and Precaspian Basin, Article, Department of Mathematics; School of Sciences and Humanities; Nazarbayev University, Academic Editor: Reza Rezaee, Published: 1 December 2021, Page 5.
62. Rubin, E.S.; Davison, J.E.; Herzog, H.J. The cost of CO₂ capture and storage. Int. J. Greenh. Gas Control 2015, 40, 378–400. [CrossRef]
63. Cardoso, J.; Silva, V.; Eusebio, D. Techno-economic analysis of a biomass gasification power plant dealing with forestry residues blends for electricity production in Portugal. J. Clean. Prod. 2019, 212, 741–753. [CrossRef]